

Plastic to Power - Microwave Energy for Plastic Decomposition



Prepared by:
Caide Marc Spietersbach

Prepared for:
Dr. Stephen Paine
Dept. of Electrical and Electronics Engineering
University of Cape Town

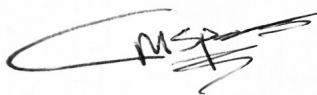
Submitted to the Department of Electrical Engineering at the University of Cape Town in partial fulfilment of the academic requirements for a Bachelor of Science degree in Electrical and Computer Engineering.

October 23, 2024

Declaration

1. I know that plagiarism is wrong. Plagiarism is to use another's work and pretend that it is one's own.
2. I have used the **IEEE** convention for citation and referencing. Each contribution to, and quotation in, this report from the work(s) of other people has been attributed and has been cited and referenced. Any section taken from an internet source has been referenced to that source.
3. This report is my own work and is in my own words (except where I have attributed it to others).
4. I have not paid a third party to complete my work on my behalf. My use of artificial intelligence software has been limited to assisting in writing (clarity and grammatical errors), formatting and LaTeX Assistance, and Code Debugging and Suggestions.
5. I have not allowed and will not allow anyone to copy my work with the intention of passing it off as his or her own work.
6. I acknowledge that copying someone else's assignment or essay, or part of it, is wrong, and declare that this is my own work.

Total Words: 17654



October 23, 2024

Caide Marc Spriestersbach

Date

Acknowledgements

Do or do not, there is no try.

—Yoda

To Trevor Norris-Jones and others at Trello Paper Company for providing the reams of thermal paper for mahala, the entire team and I who worked on this project thank and appreciate you for your contribution to the academic endeavour of creating a more sustainable future.

To my supervisor, Stephen Paine, thank you for the guidance and support throughout this project. Your knowledge and skills were invaluable to the success of this project, so was your credit card...

To Dr. Motloko Khasu, thank you for the time spent creating the catalysts, helping with the hydrogen production tests, and for the chit chats in between. I hope you continue the amazing work you're doing, and that it leads to overwhelming success.

To David Young, thank you for the years of companionship throughout this academic journey, for the coding help even on this project, for the advice and nonsense conversations along the way and for always being a stand-up human being. I cannot wait to see what you do in the future and what that might entail.

To my loving mother and father, thank you for funding me, feeding me, housing me, watering me, and dealing with my grumpiness and exhaustion not only through this project but in life in general. Quite literally, I do not know how I would be here or who I would be without you. To dad, thank you for helping out where possible with this project and teaching me everything there is to know to be good with your hands and all the knowledge that came with it – how to use tools, to measure twice and cut once, how to cast and how tie knots for fishing. To mom, thank you for the love, care, and support throughout the years. I am the man I am today because of you guys and I will forever be grateful for that.

To my brother Ross, thank you for always setting the bar so high that I was constantly pushed out of my comfort zone to become the best person I could possibly be. I have deeply appreciated the time we've spent together on the water and during boat repairs. Lucy, thank you for the advice, proof-reading, and everything beyond the work—you have been the most wonderful addition to our lives.

To my amazing girlfriend, Steph, I don't know what I would do without you. Your constant love and support, both tough and gentle, has been a guiding light for me since the day I met you. Thank you for putting up with me and sticking around. Thank you for the ear you lend when I need to offload the burdens I bear, and for the shoulder to cry on whenever I need it. I love you.

Abstract

The increasing demand for sustainable energy has driven the exploration of innovative methods for hydrogen production. This study investigates the use of microwave-assisted catalytic pyrolysis of plastics as a means of producing hydrogen, with an emphasis on the role of microplasmas and hotspot identification within microwave cavities. A key focus of the study was determining whether microplasma formation, which occurs due to localised discharges between metallic catalysts and plastic substrates, serves as the primary heating mechanism in this process.

The research was conducted using two microwave technologies: an inverter microwave and a transformer microwave, to assess how differences in energy distribution impact the efficiency and reproducibility of hydrogen production. Thermal mapping experiments were carried out to identify energy hotspots, and hydrogen production tests were performed using an FeAl_2O_3 catalyst under varying conditions.

The findings indicate that placing the catalyst in identified hotspots significantly enhances hydrogen production and consistency across tests. However, limitations such as catalyst exhaustion and equipment constraints hindered further testing. The results contribute valuable insights into the interaction between microwaves and catalysts, laying the groundwork for further investigation into microplasma formation and optimisation of microwave-assisted pyrolysis for large-scale hydrogen production.

Contents

List of Figures	ix
Glossary	xi
1 Introduction	1
1.1 Background to the Study	1
1.2 Objectives of this Study	1
1.3 Scope and Limitations	2
1.4 Plan of Development	2
2 Literature Review	3
2.1 Introduction to Microwave-Assisted Pyrolysis	3
2.1.1 Background and Context	3
2.1.2 Research Motivation and Scope	3
2.2 Theoretical Background of Microwave Heating	4
2.2.1 Electromagnetic Radiation and Microwave Spectrum	4
2.2.2 Microwave Heating Mechanism	4
2.2.3 Microwave Loss Mechanisms	5
2.2.4 Microwave Heating Characteristics	6
2.3 Microwave Waveguides, Modes, and Cavity Design	7
2.3.1 Introduction to Microwave Components and Systems	7
2.3.2 Waveguides in Microwave Systems	8
2.3.3 Microwave Modes	9
2.3.4 Cavity Design in Microwave Systems	10
2.4 Interactions Involved in Heating Metals	11
2.4.1 Electric field component (E-field)	12
2.4.2 Magnetic field component (H-field)	12
2.5 Inverter vs. Transformer Microwaves	14
2.5.1 Introduction to Inverter and Transformer Microwaves	14
2.5.2 Operational Differences and Impact on Heating	14
2.5.3 Relevance to Metal Heating and Catalysis	15
2.5.4 Relevance to Investigation	15
2.6 Application of Microwaves in Catalytic Pyrolysis of Plastics	15
2.6.1 Introduction to Microwave Pyrolysis	15
2.6.2 Application of Microwave Pyrolysis in Plastic Waste Conversion	16
2.6.3 Role of Catalysts in Microwave Pyrolysis	16
2.6.4 Challenges and Future Directions in Microwave Pyrolysis	17
2.7 Conclusion	18

3 Methodology	19
3.1 Overview of Experimental Setup	19
3.1.1 Microwave Models	19
3.1.2 Temperature Sensing Equipment	20
3.1.3 Thermal Mapping Setup	20
3.1.4 Catalyst Preparation and Testing	21
3.1.5 Experimental Workflow	21
3.2 Sensing Module Design, Calibration, and Validation	21
3.2.1 Component Selection and Module Design	21
3.2.2 Module Calibration and Testing	25
3.2.3 Thermocouple Shielding and Arcing Mitigation	27
3.2.4 Commercial Shielded Thermocouple Setup	28
3.2.5 Thermistor Placement on Microwave Cavity	29
3.2.6 Control Experiment: Water Test	29
3.2.7 Thermocouple Placement Tests with Metallic Powder	30
3.3 Thermal Mapping of Microwave Cavity	31
3.3.1 Preparation of Thermal Paper	31
3.3.2 Mode Stirrer Design and Implementation	31
3.3.3 Execution of the Test	33
3.3.4 Comparison of Results with and without Mode Stirrer	33
3.4 Hydrogen Production Testing	33
3.4.1 Materials and Equipment	34
3.4.2 Procedure	34
3.4.3 Data Collection	35
3.5 Inverter vs Transformer Hydrogen Production Test	36
4 Results	37
4.1 Temperature Sensing Module Tests	37
4.1.1 Control Experiment: Water Test	37
4.1.2 Thermocouple and FeAl ₂ O ₃ Tests	39
4.1.3 Thermocouple Placed In Powder	40
4.1.4 Thermocouple Placed with No Powder Present	41
4.2 Thermal Mapping of Inverter Microwave	42
4.2.1 1200W Thermal Mapping Test	42
4.2.2 1000W Thermal Mapping Test	43
4.2.3 700W Thermal Mapping Test	44
4.3 Thermal Mapping of Transformer Microwave	45
4.3.1 900W Thermal Mapping Test	45
4.4 Hydrogen Production Testing	46
4.4.1 Test Results and Observations	46
4.4.2 Catalyst and Plastic Mixture Testing	46
4.4.3 Hot Test Results: Hydrogen Detection	48
4.4.4 Overheating During 1000W Cold Test	48

4.4.5	Glassware Melting and Interaction with Stove Putty Holder	49
4.5	Hydrogen Production: Inverter and Transformer Microwaves	50
4.6	Summary of Key Findings	52
5	Discussion	53
5.1	Temperature Sensing Module Tests Discussion	53
5.1.1	Effectiveness of the Temperature Sensing Setup	53
5.1.2	Challenges with Thermocouple Placement	53
5.1.3	Uncertainty and Interference	53
5.1.4	Impact on Understanding of Metallic Powder Behaviour	54
5.2	Thermal Mapping Tests Discussion	54
5.2.1	Effectiveness of Thermal Mapping in Identifying Hotspots	54
5.2.2	Impact of Mode Stirrer on Heat Distribution	54
5.2.3	Fading of Heat Patterns During Successive Tests	54
5.2.4	Differences Between Power Levels	54
5.2.5	Comparison Between Inverter and Transformer Microwaves	55
5.3	Hydrogen Production Tests Discussion	55
5.3.1	Impact of Hotspots on Hydrogen Production	55
5.3.2	Power Level and Hydrogen Production	55
5.3.3	Glassware and Putty Holder Challenges	56
5.4	Hydrogen Production: Inverter vs. Transformer Microwaves	56
5.4.1	Catalyst Exhaustion and its Implications	57
5.4.2	Challenges and Limitations in Testing Setup	57
5.4.3	Dependence on External Factors and Unforeseen Constraints	57
5.5	Discussion Summary	57
6	Conclusions	58
7	Recommendations	59
7.1	Limitations and Challenges	59
7.1.1	Limitations in Catalyst Comparison	59
7.1.2	Electromagnetic Interference and Probe Uncertainty	59
7.1.3	Resistance Introduced During Soldering	59
7.1.4	Overheating and Glassware Failure	59
7.1.5	Static Nature of Thermal Mapping Tests	59
7.1.6	Variability in Microwave Technologies	60
7.2	Recommendations for Future Work	60
7.2.1	Temperature Module Improvements	60
7.2.2	Microwave Cavity and Airflow Enhancements	60
7.2.3	Thermal Mapping and Hydrogen Production Recommendations	60
7.2.4	Catalyst Comparison and Process Optimisation	61
7.2.5	Efficiency Measurement and Energy Consumption	61
7.2.6	Hydrogen Production: Inverter vs. Transformer Microwaves	61
7.3	Summary of Key Recommendations	62

Bibliography	63
8 Appendix A	68
8.1 Graduate Attribute (GA) Table	68
8.2 Use of AI in Report Writing	68
8.3 Use of AI in Report Writing	69
8.4 GitHub Repositories	71
8.5 Sensing Module Calibration and Validation Pictures	72
8.5.1 Thermocouple at the Bottom of the Cavity	72
8.5.2 Thermocouple at the Top of the Cavity	72
8.5.3 Infrared Thermogun Calibration	73
8.6 Inverter vs Transformer Additional Pictures	73
9 Appendix B	75
9.1 Ethics Forms	75

List of Figures

2.1	Diagram demonstrating transmission, reflection, and absorption of microwaves.	5
2.2	(a) Conventional heating involving heat transfer with an external heat source. (b) Microwave heating involving the conversion of microwave to thermal energy.	6
2.3	Schematic of a magnetron showing all the essential components required for the generation of microwaves, including the anode, cathode, resonant cavities, and permanent magnets. .	8
2.4	Diagram showing the differences between a rectangular waveguide and a cylindrical waveguide.	9
2.5	Diagram showing the radiation pattern of TE ₁₀	10
2.6	Figure displaying the different components which make up microwave heating	13
2.7	Comparison of power output from cycled (left) and inverter (right) microwave ovens. .	15
3.1	The web server displaying the thermistor, thermocouple, and camera feed in real time with time stamps.	23
3.2	The modified camera module for temperature monitoring, showcasing the shielding. .	24
3.3	Camera attached to the side of the microwave allowing the lens to capture information inside while having its circuitry protected.	24
3.4	A wiring diagram illustrating the connections between the MCP3008 ADC, MAX6675 thermocouple converter, and thermistors to the GPIO pins of the Raspberry Pi for the temperature sensing module.	25
3.5	Sequence of images showing the thermocouple before, during, and after the occurrence of arcing.	28
3.6	Thermocouple setup before and after the modification to reduce arcing.	28
3.7	Schematic of the microwave cavity showing the placement of thermistors (labeled 1 through 8)	29
3.8	Pictures displaying different orientations of the mode stirrers used in the experiment. .	32
3.9	The mode stirrer's installation on the turntable motor and the camera lens.	32
3.10	Flask positioned in a known hotspot before conducting the hot test.	35
4.1	Temperature readings from water control experiments at various power levels, measured by thermocouple and thermistors.	38
4.2	Temperature data from thermocouple and thermistors during the Above Powder tests at 200W for FeAl ₂ O ₃ catalyst.	39
4.3	Temperature data from thermocouple placed in FeAl ₂ O ₃ powder during 200W microwave tests.	40
4.4	Temperature vs Time for No Powder Tests at 200W	41
4.5	Thermal mapping results at 1200W power level. Top row: heating patterns before the mode stirrer insertion. Bottom row: heating patterns after the mode stirrer insertion. .	42
4.6	Thermal mapping results at 1000W power level. Top row: heating patterns before the mode stirrer insertion. Bottom row: heating patterns after the mode stirrer insertion. .	43

4.7 Thermal mapping results at 700W power level. Top row: heating patterns before the mode stirrer insertion. Bottom row: heating patterns after the mode stirrer insertion.	44
4.8 Thermal mapping results for the Transformer microwave. Top row: heating patterns before the mode stirrer was inserted. Bottom row: heating patterns after the mode stirrer insertion.	45
4.9 Visuals of the catalyst and plastic during the heating stages of hydrogen production tests.	47
4.10 Hydrogen bubbles detected during hot tests at various power levels.	48
4.11 Temperature readings from the 1000W cold test showing significant overheating.	48
4.12 Round-bottom flask heating during high-power tests.	49
4.13 Post-test damage to the glass and stove putty holder.	50
4.14 Hydrogen production results from inverter microwave runs using reduced FeAl ₂ O ₃ catalyst.	51
8.1 Example of AI providing assistance with clarity and grammar improvements.	69
8.2 Example of AI assisting with LaTeX formatting for a chapter title and spacing issues.	70
8.3 Example of AI providing suggestions and debugging help for code used in the project.	71
8.4 Temperature profiles with thermocouple placed at the bottom of the cavity (200W, FeAl ₂ O ₃ catalyst).	72
8.5 Temperature profiles with thermocouple placed at the top of the cavity (200W, FeAl ₂ O ₃ catalyst).	72
8.6 Non-Contact Industrial Infrared Thermometer displaying a reading used to confirm the thermocouple calibration during the experiment.	73
8.7 Additional experimental setups and catalyst condition.	74

Glossary

ADC Analog-to-Digital Converter

bimetallic catalyst A catalyst composed of two different metals, often used in microwave pyrolysis to enhance reaction selectivity and efficiency

catalyst A substance that increases the rate of a chemical reaction without undergoing any permanent change itself

electromagnetic wave Energy that propagates through space as oscillating electric and magnetic fields at the speed of light

EMI Electromagnetic Interference

HDPE High-Density Polyethylene

high-density polyethylene A type of plastic used in hydrogen production experiments

magnetron A diode-type electron tube responsible for generating microwaves in microwave systems

MAP Microwave-Assisted Pyrolysis

microwave Electromagnetic radiation with wavelengths ranging from 0.01 to 1 meters, used for heating in MAP processes

pyrolysis Thermal decomposition of organic materials in the absence of oxygen, producing char, oil, and gas

RADAR Radio Detection and Ranging

TE Transverse Electric mode, a mode in which the electric field is perpendicular to the direction of wave propagation

TEM Transverse Electromagnetic mode, a mode in which the electric and magnetic fields are both perpendicular to the direction of wave propagation

TM Transverse Magnetic mode, a mode in which the magnetic field is perpendicular to the direction of wave propagation

waveguide A waveguide is a rectangular or circular pipe, usually made of copper, that confines and guides very high-frequency electromagnetic waves between two locations

Chapter 1

Introduction

1.1 Background to the Study

The increasing global demand for cleaner energy sources has driven significant research into hydrogen as a potential alternative fuel. Hydrogen is considered a key component in the transition to a low-carbon economy due to its high energy density and zero greenhouse gas emissions when used in fuel cells [1]. A promising method for hydrogen production is microwave-assisted catalytic pyrolysis, which involves the thermal decomposition of materials, such as plastics, in the presence of a catalyst. This technique offers a cleaner and more efficient way to produce hydrogen compared to traditional methods, while also generating valuable by-products such as carbon nanotubes [2].

Carbon nanotubes, produced during the pyrolysis of plastics, are highly valuable materials due to their exceptional mechanical, electrical, and thermal properties [3]. Their simultaneous production with hydrogen makes microwave-assisted catalytic pyrolysis an even more attractive approach, contributing to both energy generation and the creation of high-value nanomaterials. This dual benefit underscores the importance of further understanding and optimising this process.

Microwave-assisted reactions provide unique advantages due to the selective heating of materials, offering energy efficiency and control over reaction conditions. However, understanding the mechanisms by which microwaves interact with catalysts, and ensuring consistent and reproducible results, remains a challenge. One emerging hypothesis is that microplasmas (small, localised discharges that form between metallic particles and plastic substrates) could be responsible for initiating the heating process, particularly microwave-absorbing catalysts such as FeAl_2O_3 . These microplasmas could create localised hotspots that lead to catalytic reactions, ultimately producing hydrogen and carbon nanotubes.

In this context, it is critical to investigate how different microwave technologies (inverter vs. transformer) and energy distributions within the microwave cavity affect the reproducibility and efficiency of hydrogen and carbon nanotube production. This study aims to test the hypothesis that placing a FeAl_2O_3 catalyst mixture in identified microwave hotspots will enhance the consistency and yield of hydrogen production. Furthermore, the study seeks to explore whether microplasma formation is indeed the heating mechanism driving these reactions.

1.2 Objectives of this Study

This study addresses three main research questions. First, it investigates whether microplasma formation serves as the primary heating mechanism in [Microwave-Assisted Pyrolysis \(MAP\)](#) when using FeAl_2O_3 as a catalyst. Second, it explores the potential of using thermal mapping to identify reproducible hotspots within the microwave cavity, hypothesising that placing the catalyst in these hotspots will improve hydrogen production efficiency. Third, it examines the effects of different

microwave technologies, specifically inverter and transformer microwaves, on energy distribution and the yield of hydrogen production.

The purpose of this study is to deepen the understanding of microwave-assisted catalytic reactions for hydrogen production, particularly by exploring the role of microplasmas and energy distribution within microwave cavities. The research addresses two key challenges in this field: ensuring reproducibility in hydrogen production and identifying the optimal conditions under which catalysts can perform most efficiently.

1.3 Scope and Limitations

This research focuses on the use of microwave-assisted catalytic pyrolysis to produce hydrogen from a mixture of FeAl_2O_3 catalyst and High-Density Polyethylene (HDPE) plastic. The experiments were conducted in two types of microwave ovens: an inverter microwave and a transformer microwave, to assess their respective effects on reaction efficiency and reproducibility. The scope of the study includes thermal mapping to identify energy hotspots within the microwave cavity, followed by hydrogen production tests conducted in both hotspot and non-hotspot conditions.

Several limitations impacted the study. The experiments were constrained by time and the availability of fresh catalyst material, which prevented further testing. Additionally, the equipment available could not directly capture microplasmas during the experiments, relying instead on indirect evidence through thermal mapping and temperature data.

1.4 Plan of Development

The structure of this report follows the logical progression of the research and reflects the development of the study's key findings. Chapter 2 begins with a comprehensive overview of the existing research on microwave-assisted hydrogen production, highlighting the relevant advancements and gaps in the literature. Chapter 3 then describes the experimental approach, detailing the design of the temperature sensing module, the thermal mapping procedures, and the hydrogen production tests. The results are presented in chapter 4, where the performance of the FeAl_2O_3 catalyst under different conditions is evaluated, alongside the outcomes of the temperature monitoring and thermal mapping tests. Chapter 5 delves into the interpretation of these findings, discussing the significance of hotspot identification within the microwave cavity and exploring the role of microplasmas in the catalytic processes. Finally, the conclusions in chapter 6 provide a summary of the experimental outcomes, while chapter 7 offers recommendations for future research and further optimisation of the experimental setup.

Chapter 2

Literature Review

This chapter aims to explore the fundamental principles and advancements in MAP, with a particular focus on its application in plastic waste management and energy production. This literature review covers various aspects of microwave heating, including its underlying mechanisms, the role of catalysts, and the advantages of MAP over conventional pyrolysis techniques. The objective is to provide a comprehensive understanding of how microwave technology can enhance the efficiency and scalability of pyrolysis processes, especially in the context of sustainable waste conversion. By reviewing recent studies and experimental results, this chapter also identifies key challenges and opportunities for further research.

2.1 Introduction to Microwave-Assisted Pyrolysis

2.1.1 Background and Context

Pyrolysis is a thermal decomposition process in which materials are broken down at elevated temperatures in the absence of oxygen, resulting in the production of bio-oil, char, and gases [4]. Traditionally, pyrolysis has relied on external heat sources to initiate and sustain the process, but recent advancements have introduced microwave technology as a more efficient alternative. Microwave pyrolysis employs microwave heating to convert biomass, waste, and other organic materials into valuable products such as oil, char, and gases [5]. This technique offers several advantages over conventional pyrolysis, including in-core volumetric heating, which allows for more uniform temperature distribution throughout the material, overcoming limitations related to reactor design and raw material particle size [5].

MAP enhances the process by integrating microwave technology with traditional pyrolysis methods, facilitating faster heating rates, higher energy utilisation, and increased selectivity in product formation [4]. The development of MAP marks a significant advancement in pyrolysis technology, addressing inefficiencies present in conventional methods and expanding the range of materials that can be effectively processed. In 1968, Fu et al. demonstrated that MAP of high-volatile bituminous coal in the presence of nitrogen produced valuable compounds, including hydrogen cyanide, acetylene, and low molecular weight hydrocarbons [6]. One of the earliest applications of pyrolysis for waste management was a plant built in the United Kingdom in 1989, designed to break down the polymers found in tires [7]. Since then, the field has evolved considerably, with MAP emerging as a promising technique for sustainable waste conversion and energy production.

2.1.2 Research Motivation and Scope

Despite the advantages of MAP, several challenges and knowledge gaps remain that hinder its broader adoption and optimisation. One significant issue is the economic feasibility of MAP, particularly concerning the initial investment and operational costs involved in scaling the technology for industrial applications [8]. Additionally, most studies conducted on MAP focus on batch operation modes and

2.2. Theoretical Background of Microwave Heating

frequently rely on microwave absorbers to prevent hotspots and enhance process efficiency [9]. However, while absorbers help control heating, they also reduce the temperature threshold for the temperature runaway effect, raising concerns about their scalability for industrial biofuel production [9].

A critical gap in the literature is the limited understanding of the dielectric properties of materials subjected to MAP, which determine the material's ability to convert microwave energy into heat [10]. These properties are not always well understood or known for various materials [10]. Furthermore, the operating conditions and parameters that govern the efficiency of MAP are not fully optimised, making it difficult to scale the process with consistent results [10]. This gap is central to this study, which aims to explore how microwave interactions with different catalysts influence reaction chemistry and kinetics [5].

Additionally, unique phenomena associated with microwave heating, such as the formation of hotspots and microplasmas, require further investigation to improve control and testing of MAP processes [5]. These phenomena are critical for developing more effective microwave reactor designs and ensuring uniform heating [5]. Another key challenge is the inherent difficulty of achieving accurate temperature measurement and uniform heating in microwave reactors, as current systems often lack real-time, multi-zone temperature monitoring, which could reveal significant temperature variations within the sample during pyrolysis [5, 11].

Furthermore, current research on MAP typically does not explore the influence of different microwave technologies, cavity sizes, or operating modes. Studies also often operate at lower microwave power levels, typically around 800W, reaching temperatures of only 500°C, while higher wattages and alternative microwave setups may offer opportunities for improved performance [2, 5]. These gaps in the existing literature underscore the need for further research into how these factors influence MAP processes. This investigation will address these areas by examining the effects of microwave power levels, catalyst properties, and reactor design on the efficiency and scalability of MAP.

2.2 Theoretical Background of Microwave Heating

2.2.1 Electromagnetic Radiation and Microwave Spectrum

Electromagnetic radiation, as described by Maxwell's electromagnetic theory, is energy that travels in the form of electromagnetic waves at the speed of light [12]. These waves consist of oscillating magnetic and electric fields propagating at right angles to each other [12]. Microwave frequencies typically range from 300MHz to 300GHz on the electromagnetic spectrum, with corresponding wavelengths of 0.01m to 1m, falling between the radio and infrared regions [13]. The microwave spectrum is widely used for applications such as Radio Detection and Ranging (RADAR) transmission and telecommunications, with frequencies of 900MHz and 2.45GHz commonly employed in industrial and domestic microwave ovens to prevent interference with other technologies [14].

2.2.2 Microwave Heating Mechanism

Microwave heating converts electromagnetic energy into heat, providing an efficient alternative to traditional conductive heating mechanisms [14]. The way this energy is distributed and absorbed

depends on how the material interacts with the electromagnetic radiation, including processes like transmission, reflection, or absorption. Figure 2.1 illustrates these interactions [15].

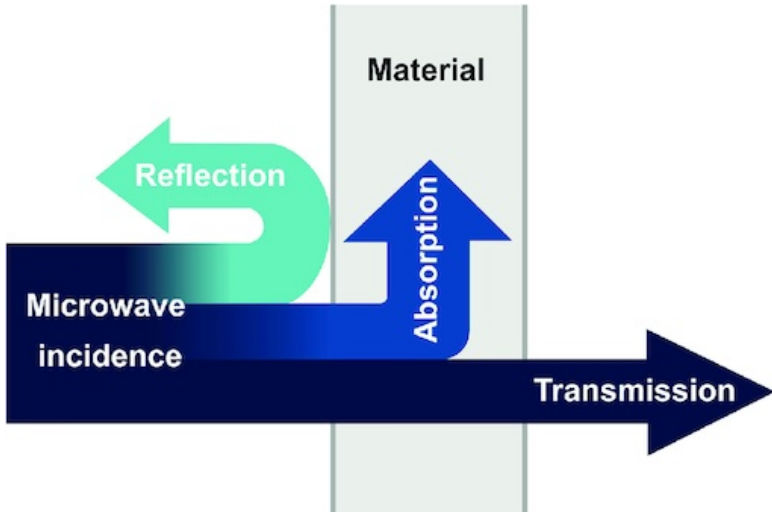


Figure 2.1: Diagram demonstrating transmission, reflection, and absorption of microwaves.

Image Source: [15]

Materials can be broadly classified into three categories based on their interaction with microwaves:

- **Transmissive Materials:** These are non-metallic materials that allow microwaves to pass through without significant energy alteration [15].
- **Reflective Materials:** Metals fall into this category, reflecting the incident microwave energy [15].
- **Absorptive Materials:** These materials neither reflect nor transmit microwaves; instead, they absorb the energy, requiring good impedance matching and strong microwave loss characteristics [15].

2.2.3 Microwave Loss Mechanisms

The efficiency of microwave heating is heavily influenced by two types of loss mechanisms: **dielectric loss** and **magnetic loss**. These mechanisms determine how well a material can convert microwave energy into heat [15].

Dielectric Loss includes conductive loss, interface polarisation, and dipole polarisation. Dielectric loss occurs in polar materials where molecular dipoles try to align with the oscillating microwave field, generating heat due to friction between molecules [15]. **Magnetic Loss** is a type of loss which includes phenomena such as hysteresis, loss, and natural resonance. Magnetic materials, particularly ferrites and magnetic metal particles like Fe, Ni, and Co, experience magnetic losses due to the interaction between the magnetic component of the microwaves and the magnetic domains of the material [15].

Materials with high dielectric loss, such as ceramics and carbon-based materials, are more efficient in converting microwave energy into heat. Conversely, magnetic loss is critical for magnetic metals and

alloys, which can absorb significant microwave energy through these mechanisms.

2.2.4 Microwave Heating Characteristics

Microwave heating is non-contact and volumetric, meaning that [electromagnetic waves](#) penetrate materials and generate heat from within, as opposed to conventional methods where heat is conducted from an external source [15]. This difference allows for more efficient and uniform heating, especially in cases where internal heat generation is desired. Figure 2.2 illustrates the comparison between conventional and microwave heating mechanisms.

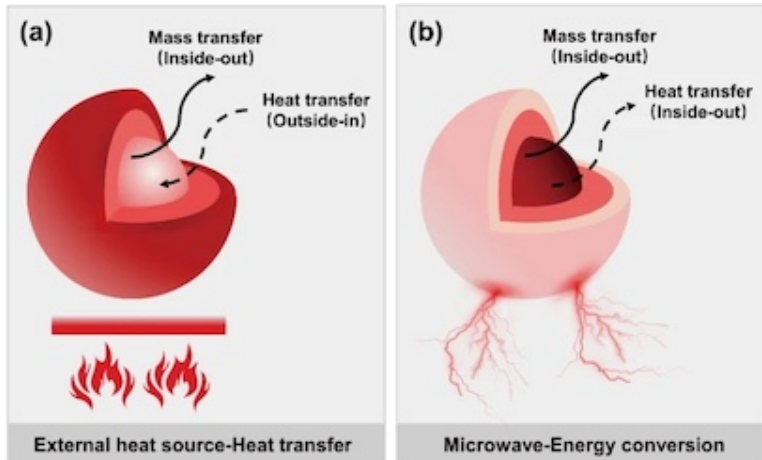


Figure 2.2: (a) Conventional heating involving heat transfer with an external heat source. (b) Microwave heating involving the conversion of microwave to thermal energy.

Image Source: [15]

The most notable feature of microwave heating is its ability to achieve selective heating, where energy is concentrated in specific areas based on the material's composition, leading to efficient overlap between thermal zones and reaction sites [15]. This enables microwave systems to heat materials more uniformly and rapidly than conventional heating methods.

Microwave absorption capability is commonly quantified by the loss angle tangent ($\tan\delta$), which measures how effectively a material absorbs microwave energy [16]. Materials with $\tan\delta$ greater than 0.5 are considered strong microwave absorbers, while those with values less than 0.1 are weak absorbers [16].

The principles of microwave heating, including dielectric and magnetic loss, highlight its superiority over conventional heating methods in terms of volumetric and selective heating. These principles form the foundation for understanding how microwaves interact with different materials, particularly in the context of pyrolysis. Optimising the interaction between microwaves and materials is crucial for improving the efficiency of [MAP](#). This theoretical foundation is essential as it informs the subsequent exploration of catalysts and reaction efficiency in microwave-based systems.

2.3 Microwave Waveguides, Modes, and Cavity Design

2.3.1 Introduction to Microwave Components and Systems

The efficiency of MAP is heavily influenced by the design of the microwave system, including the type of microwave mode, waveguide design, and cavity configuration. These factors determine how microwaves are distributed within the reactor, impacting the uniformity of heating and, ultimately, the efficiency of the pyrolysis process. The proper design of the microwave system ensures that the energy is evenly distributed across the material being processed, minimising the formation of hotspots and cold spots.

At the heart of any microwave system is the magnetron, the primary component responsible for generating microwaves. The magnetron is a diode-type electron tube composed of an anode, cathode, antenna, and high-power permanent magnets. By applying high voltage electricity, the magnetron produces microwaves, which are transmitted from the microwave generator to the reactor chamber through waveguides [9]. Understanding the operation of the magnetron is essential, as it directly influences the characteristics of the microwaves generated, which in turn affects how the microwaves interact with materials in the pyrolysis process.

The magnetron is responsible for converting electrical energy from a low-frequency power source into high-frequency electromagnetic energy, specifically microwaves [17]. This device consists of a metal cylinder that acts as the anode, with several resonant cavities positioned radially around a central cavity, where a titanium filament serves as the cathode (Figure 2.3) [17]. When high voltage is applied, the filament heats up and emits electrons through thermionic emission, with the negatively charged electrons being drawn towards the positively charged anode [17]. Positioned between strong magnetic fields, the movement of electrons through the interaction space (between the anode and cathode) is influenced by the electric and magnetic fields [17]. This causes the electrons to move in circular trajectories around the resonant cavities, producing microwaves as a result of the electromagnetic oscillations they generate. The frequency of the emitted microwaves is determined by the size and configuration of the cavities [17].

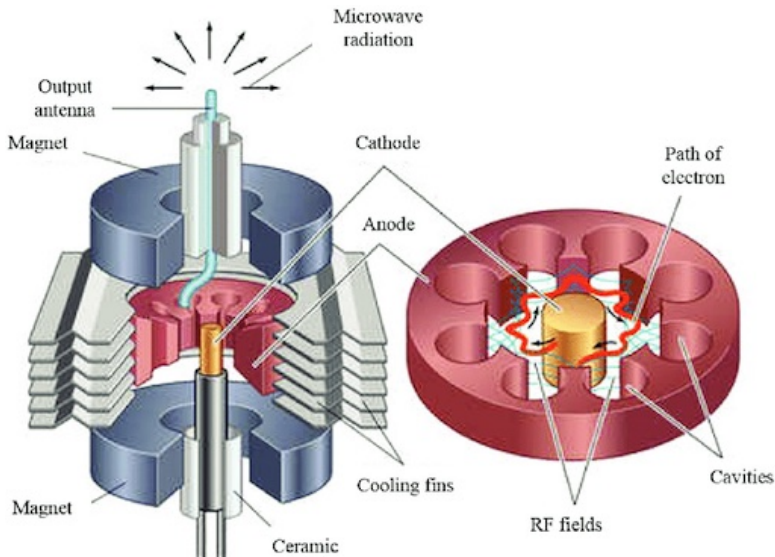


Figure 2.3: Schematic of a magnetron showing all the essential components required for the generation of microwaves, including the anode, cathode, resonant cavities, and permanent magnets.

Image Source: [17].

2.3.2 Waveguides in Microwave Systems

Introduction to Waveguides

Waveguides are essential components of microwave systems, functioning as conduits to transmit microwaves from the generator, typically a magnetron, to the application chamber or reactor cavity [18]. Their primary role is to direct microwave energy efficiently into the reactor, minimising energy losses and ensuring uniform propagation of microwaves through the material being processed [19]. In MAP, the design and positioning of waveguides are critical for ensuring that microwave energy interacts effectively with the material inside the reactor, maximising heating efficiency.

Types of Waveguides

Various types of waveguides are employed in microwave systems, each offering unique properties that influence how microwaves are transmitted and distributed. The most commonly utilised type in industrial microwave heating is the **rectangular waveguide**, which is preferred for its ability to transmit microwaves with minimal loss and high power efficiency [20, 21]. The design of rectangular waveguides supports specific modes of microwave propagation, which are determined by the waveguide's dimensions and the frequency of the microwaves being transmitted [22].

In some cases, **circular waveguides** are also used, although they are less prevalent compared to rectangular waveguides [20]. Circular waveguides have certain advantages, such as supporting multiple propagation modes, but their analysis and application can be more complex [20, 23]. The selection of the waveguide's shape and material is dictated by the system's requirements, such as the need for high power transmission and minimal energy loss [23].

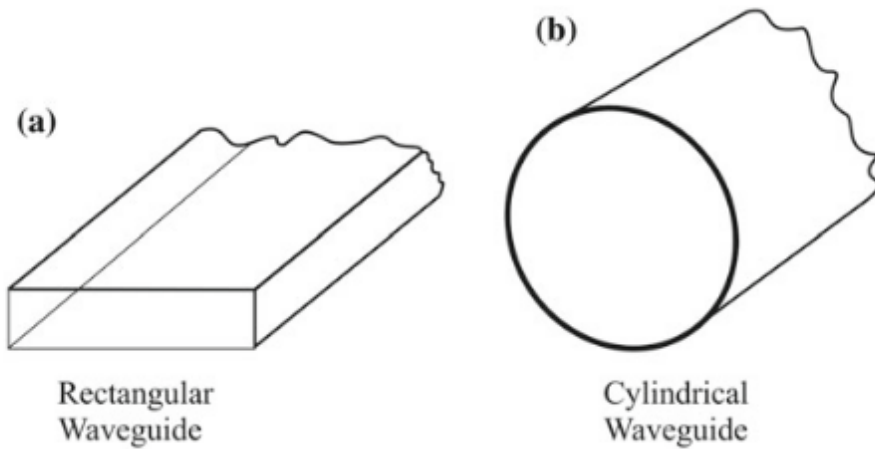


Figure 2.4: Diagram showing the differences between a rectangular waveguide and a cylindrical waveguide.

Image Source: [24].

2.3.3 Microwave Modes

Introduction to Microwave Modes

In microwave systems, the concept of **modes** refers to the patterns of the electric and magnetic fields as microwaves propagate through [waveguides](#) or reactor cavities. These modes determine how the microwave energy is distributed across the material being processed. The way these fields interact with the material is crucial for ensuring uniform heating, as different modes can lead to variations in field intensity, resulting in hot spots or cold spots [25]. Proper mode selection and management are essential in [MAP](#) to achieve efficient and uniform heating.

Transverse Electric and Transverse Magnetic Modes

In transmission line theory, microwaves are often described by the Transverse Electromagnetic (**TEM**) wave, which propagates in the z -direction. In this mode, the electric field is aligned along the x -axis, and the magnetic field is aligned along the y -axis, meaning that neither the electric nor magnetic field has components in the direction of wave propagation [24]. However, in the case of waveguides, other wave modes become more relevant, specifically **Transverse Electric (TE)** modes and **Transverse Magnetic (TM)** modes [24].

For **TE** waves, the electric field is entirely perpendicular to the direction of wave propagation, while the magnetic field has components along the propagation direction [24]. In this case, there is no electric field component in the direction of wave propagation [24]. Conversely, in **TM** waves, the magnetic field is perpendicular to the direction of propagation, and the electric field has components along the wave's direction of travel [24]. There is no magnetic field component in the direction of wave propagation [24]. While **TEM** waves can propagate at any frequency, **TE** and **TM** waves can only propagate within a waveguide when the frequency of the [electromagnetic wave](#) exceeds a threshold known as the cut-off frequency [24].

The modes are typically represented as TE_{mn} or TM_{mn} , where the subscript m refers to the number of half-wave variations of the electric field (or the magnetic field in the case of TM modes) along the wider dimension of the waveguide, denoted as a in the x -direction [26]. Similarly, n indicates the number of half-wave variations across the narrower dimension, denoted as b in the y -direction, see Figure 2.5 [26].

A rectangular waveguide can support an infinite number of TM modes for each integer value of m and n , and they are denoted by TM_{mn} [20]. However, if either m or n is zero, no field will exist in the waveguide [20]. In rectangular waveguides, the TE_{10} and TM_{11} modes are the dominant modes, as they have the lowest cut-off frequencies, allowing them to propagate more easily compared to higher-order modes [26].

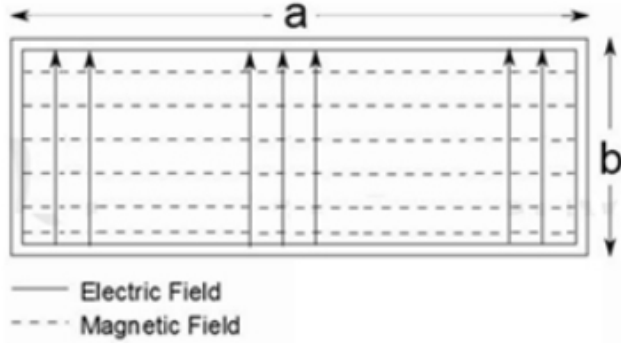


Figure 2.5: Diagram showing the radiation pattern of TE_{10} .

Image Source: [26].

Higher-Order Modes

As the frequency of the microwaves increases, higher-order modes can be excited. The dominant mode typically offers low loss and distortion free transmission, while higher-order modes tend to result in significant power loss [26]. In **MAP** systems, the presence of higher-order modes can cause non-uniform heating, which may negatively affect the process efficiency. Managing these modes through proper waveguide design and mode converters can help mitigate these effects.

2.3.4 Cavity Design in Microwave Systems

Introduction to Microwave Cavities

In **microwave** systems, the cavity is the enclosed space where microwaves interact with the material being processed. The design of the cavity plays a critical role in determining how microwave energy is distributed throughout the material, affecting the efficiency and uniformity of heating. The size, shape, and dimensions of the cavity influence the type of modes that can propagate, which in turn affects how microwaves are absorbed by the material [27]. Proper cavity design is essential in **MAP** systems to ensure that energy is transmitted efficiently and that hot spots or cold spots are minimised [27].

Single-Mode vs. Multi-Mode Cavities

Microwave cavities can generally be classified into two categories: **single mode cavities** and **multi-mode cavities**. Multi-mode cavities are more commonly used for processing bulk materials or larger arrays of discrete materials. These materials often have dimensions larger than the wavelength of the operating frequency, making them unsuitable for single-mode cavities. Multi-mode cavities, such as those found in household microwave ovens, are typically metal enclosures excited at a frequency well above their fundamental cutoff frequency [28].

For example, a common home microwave oven has internal dimensions of around 12 inches ($\approx 30\text{cm}$) to 16 inches ($\approx 41\text{cm}$), compared to a wavelength of about 4.8 inches ($\approx 12\text{cm}$) [28]. Since the cavity dimensions are significantly larger than the microwave wavelength, a large number of standing-wave modes can exist near the operating frequency [28]. This allows multi-mode cavities to excite multiple modes simultaneously, which helps to minimise heating non-uniformity even when field-perturbing materials are present inside the cavity [28]. Important considerations in multi-mode applicator design include achieving uniform heating, determining the required microwave power, and controlling leakage suppression and performance characteristics [28].

In contrast, single mode cavities typically consist of a [waveguide](#) section operating near the cutoff frequency. These cavities are product-specific and often have holes or slots to allow materials to enter or exit the cavity [28]. While single mode cavities offer more focused heating, they can be highly sensitive to changes in the properties, geometry, or position of the material being processed, which may result in detuning the applicator from resonance [28]. This sensitivity makes single-mode cavities more complex and expensive to design, often requiring automatic controls and feedback systems to maintain optimal performance [28]. Due to these limitations, single mode cavities are less commonly used for general-purpose applications and are more suited to specific, controlled processes [28].

The understanding of [microwave](#) modes, [waveguides](#), and cavity design is crucial in optimising [MAP](#) systems. Each component significantly affects the uniformity and efficiency of heating. The choice of waveguides and their configuration influences how microwaves are directed and distributed, which is essential in achieving effective energy transmission. The modes of propagation within the waveguides, such as **TE** and **TM** modes, play a key role in determining the field intensity and uniformity across the material. Finally, the design of the cavity, whether single mode or multi-mode, impacts the excitation of modes and the resultant heating patterns. Since non-uniform heating can lead to inconsistent [pyrolysis](#) reactions, understanding these factors is fundamental to investigating how microwaves interact with [catalysts](#) and metals, which directly relates to the scope of this research.

2.4 Interactions Involved in Heating Metals

Microwaves interact with materials in distinct ways depending on their dielectric and magnetic properties. Metals, due to their high electrical conductivity, are generally considered reflective to microwaves, which prevents electromagnetic fields from penetrating them [12]. However, under certain conditions, such as in powder form or thin films, metals can absorb microwave energy and convert it into heat [12]. This discovery has opened new opportunities for metal processing, such as microwave-assisted sintering, joining, and melting [12].

Unlike dielectric materials, which primarily rely on dipole polarisation and ionic conduction for microwave absorption, metals exhibit significant magnetic losses [29]. These losses, such as eddy current formation, hysteresis, and magnetic induction heating, dominate the heating of metallic materials [29]. The efficiency of microwave absorption in metals depends on the microwave operating frequency, the size and shape of the metal particle and the electromagnetic properties of the metal [30]. Recent studies have also observed phenomena like microwave-induced discharges and plasma formation at sharp edges or irregular surfaces of metals, which result in localised heating and material property changes that are unattainable with traditional methods [31].

2.4.1 Electric field component (E-field)

Dielectric Polarisation

Microwave heating occurs when the electric field causes charges in a material to become polarised, though this polarisation cannot keep up with the rapid reversals of the field [14]. The total polarisation consists of four components: electronic, atomic, dipole, and interfacial polarisation [14].

1. **Electronic Polarisation:** Caused by the displacement of valence electrons around nuclei [12].
2. **Atomic Polarisation:** The displacement of positive and negative ions or atoms from their equilibrium position [12].
3. **Dipolar Polarisation:** Permanent dipole moments in molecules that reorient under the influence of an alternating electric field [12].
4. **Interfacial Polarisation:** Charges accumulating at material boundaries, also referred to as the Maxwell-Wagner effect [14].

Since electronic and atomic polarisation occur on much faster timescales than microwave frequencies, they do not significantly contribute to heating [14]. The slower dipolar and interfacial polarisation components are primarily responsible for determining the dielectric properties of materials at microwave frequencies, causing continuous orientation and disorientation as the field oscillates [14].

Ionic Conduction Losses

Conduction losses in metals arise when free electrons or ions in the material move back and forth in response to the oscillating electric field, creating electric currents and generating heat through resistive losses [29]. This effect is particularly prominent in high-conductivity metals, where the motion of charge carriers dominates the heating process [29].

2.4.2 Magnetic field component (H-field)

Understanding the role of the magnetic field (H-field) in microwave heating has been a significant focus in various studies. Research has shown that certain metals, particularly powders of copper (Cu), tungsten (W), iron (Fe), and cobalt (Co), absorb significantly more microwave energy in the H-field than in the electric field (E-field) [32][33]. This results in faster temperature increases in the presence of the magnetic field [32]. These findings underscore the contribution of magnetic losses, such as eddy currents and hysteresis, in the microwave heating of metals [29].

Eddy Current Losses

In the presence of a magnetic field, eddy currents are induced in conductive materials due to the interaction between the field and the metal [29]. These circulating currents form near the surface of the material due to the skin effect, where current density decreases with depth, leading to localised heating [12].

In insulating materials like ceramics, conduction losses are minimal at room temperature due to low conductivity. However, as temperature rises, conductivity increases, improving the material's ability to absorb microwave energy by enhancing its dielectric properties [12].

Hysteresis Losses

Hysteresis losses occur when magnetic materials are subjected to an alternating magnetic field, resulting in energy dissipation as heat [12]. The energy loss per cycle corresponds to the area within the hysteresis loop, which plots magnetic flux density (B) against magnetising force (H) [12]. Significant hysteresis losses are seen in ferrous magnetic materials when exposed to an alternating magnetic field [29].

Magnetic Resonance Losses

Magnetic resonance losses occur when the frequency of the applied electromagnetic field matches the natural oscillation frequency of a material's magnetic dipoles [34]. This resonant effect can cause rapid heating, particularly in ferromagnetic materials [34].

Residual Losses

Residual losses, as described by Buschow, include rotational resonance and domain wall resonance, mechanisms in which magnetic dipoles and domain walls move in response to an oscillating magnetic field [35]. These additional losses contribute to the heating of magnetic materials but are generally smaller compared to eddy currents and hysteresis [14].

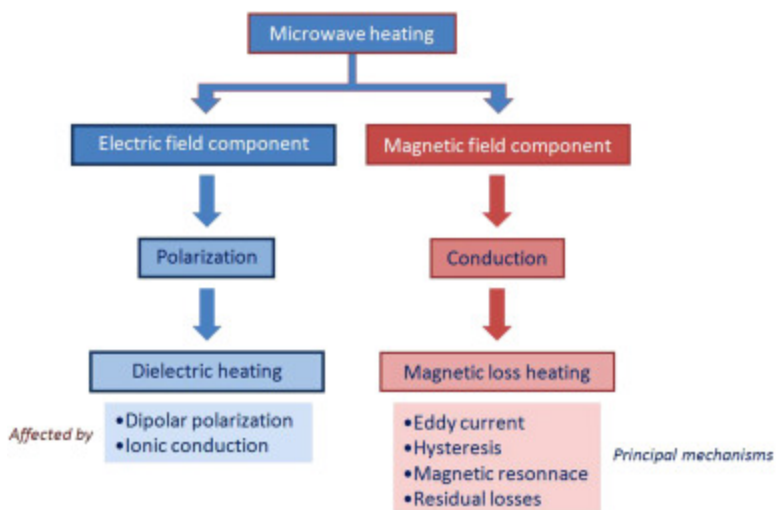


Figure 2.6: Figure displaying the different components which make up microwave heating

Image Source: [36]

Figure 2.6 shows the components involved in microwave heating, including dielectric heating, conduction, and magnetic losses. For this project, understanding these mechanisms is key to optimising catalyst design and ensuring efficient conversion during pyrolysis.

Microwave interactions with metals, particularly the mechanisms involving magnetic losses such as eddy currents and hysteresis, are based on theoretical models that have yet to be fully proven in practical applications. These theories suggest that metals, especially in powdered or thin-film forms, can absorb microwave energy under certain conditions, but the exact nature of this interaction requires further investigation. In this project, understanding why and how microwaves interact with different metals is essential for identifying the most effective catalysts. By examining factors such as particle size, composition, and the microwave operating conditions, this research aims to validate these theories and optimise catalyst selection for enhanced performance in microwave systems.

2.5 Inverter vs. Transformer Microwaves

2.5.1 Introduction to Inverter and Transformer Microwaves

Microwave ovens generally operate using one of two power delivery methods: inverter-based or transformer-based (cycled) microwaves. **Transformer-based microwaves** are the more traditional design, where the magnetron operates at full power for short bursts, followed by periods of no power. This cyclical on-off pattern delivers the time-averaged power but often leads to fluctuations in temperature due to the repeated cooling phases [37]. In contrast, **inverter-based microwaves** employ continuous power output, allowing for more precise control over the heating process by maintaining a constant power level, theoretically improving heating uniformity and efficiency [37, 38].

2.5.2 Operational Differences and Impact on Heating

Transformer-based microwaves, due to their pulsing nature, can lead to uneven heating, particularly at the edges and corners of materials, where the temperature tends to increase rapidly [37]. This is attributed to the heat conduction that occurs during the power-off phases, allowing heat to diffuse from hot spots to cooler regions [39]. In contrast, inverter-based microwaves provide a more steady power supply, which reduces temperature fluctuations during heating, but may not always improve uniformity significantly, as has been reported by Panasonic [37]. These differences in technologies are shown in Figure 2.7

In MAP, the impact of these operational differences on metal catalysts has not been fully explored. While food studies indicate that cycled power can improve heating uniformity by allowing more time for heat conduction, the effect on materials like metals or catalysts, which behave differently from food, remains unclear [39]. Inverter microwaves, by providing continuous power, might offer better control over the heating process in certain materials but may not resolve issues like ‘thermal runaway’ or non-uniform electric field distributions [37].

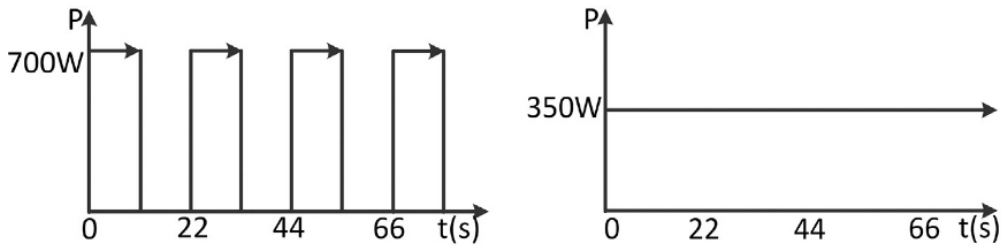


Figure 2.7: Comparison of power output from cycled (left) and inverter (right) microwave ovens.

Image Source: [37].

2.5.3 Relevance to Metal Heating and Catalysis

Although most of the existing literature focuses on the heating of food products, the principles of inverter and transformer (cycled) heating can be extrapolated to metal catalysts. The influence of factors like size, granularity, and material properties of catalysts is expected to play a significant role in how microwaves interact with metals under these different heating modes. While cycled microwaves may allow heat to conduct through metal powders during the off-cycles, leading to more uniform heating, inverter-based systems could provide more consistent heating rates, particularly in materials that require precise temperature control. However, as noted in food studies, these differences may not be as pronounced unless the material's electromagnetic properties differ significantly [37].

This investigation seeks to address the gaps in the current understanding of how these microwave technologies interact with metals, particularly in MAP. The literature suggests that heating performance can vary depending on the characteristics of the material being processed, and this research will explore how catalysts behave under cycled and inverter microwave heating. This is especially important given the limited availability of literature on this subject, highlighting the novelty and significance of this study.

2.5.4 Relevance to Investigation

There is limited literature available comparing the interaction of cycled and inverter microwave heating with metals, particularly in the context of pyrolysis. Most studies have focused on food products, where both heating methods have been shown to deliver similar time-averaged power, but with varying impacts on heating uniformity depending on material properties and oven configurations [37]. In the case of metals and catalysts, this research aims to fill the gap in understanding how these different heating methods affect their interaction with microwaves, building on principles derived from related fields to investigate this phenomenon comprehensively.

2.6 Application of Microwaves in Catalytic Pyrolysis of Plastics

2.6.1 Introduction to Microwave Pyrolysis

MAP is a thermochemical process that uses microwave energy to decompose materials, such as plastics, in the absence of oxygen. Compared to conventional pyrolysis methods, which rely on external

heating, microwave pyrolysis provides rapid and volumetric heating, leading to more efficient and faster decomposition of feedstock [15]. The efficiency of microwave pyrolysis makes it an attractive solution for plastic waste management, as it allows for the conversion of plastic into valuable by-products like hydrogen and carbon nanotubes, aiding in the development of a sustainable circular economy [2].

2.6.2 Application of Microwave Pyrolysis in Plastic Waste Conversion

One of the primary applications of microwave pyrolysis is the up-cycling of plastic waste. Plastic, composed of long-chain polymers, is broken down into smaller molecules, such as hydrogen and carbon nanotubes, through MAP [2]. Recent research has shown that bimetallic catalysts, such as $\text{Ni}_3\text{Co}_2\text{O}_x$, can convert the electromagnetic wave energy from microwaves into heat, initiating the dehydrogenation of plastics [2]. The selective heating of these catalysts under microwave radiation makes them highly effective for the up-cycling process, even with landfill-mixed plastics, which do not require pretreatment [2].

In comparison to conventional thermal catalytic dehydrogenation processes, microwave-assisted methods demonstrate greater energy efficiency, with a study showing that microwave pyrolysis of plastic using $\text{Ni}_3\text{Co}_2\text{O}_x$ achieved energy efficiency three times higher than electric furnace heating [2]. This suggests that microwave pyrolysis not only accelerates the reaction process but also reduces the overall energy consumption. Furthermore, the use of catalysts that can absorb microwaves efficiently plays a key role in ensuring that the process operates at lower temperatures and under less intensive conditions, leading to higher yields of valuable products [2].

The performance of MAP depends on various factors, including the microwave power and the type of catalyst used. For instance, experiments with $\text{Ni}_3\text{Co}_2\text{O}_x$ have demonstrated optimal reaction conditions at 800 W and 500 °C [2]. These findings highlight the importance of catalyst selection and process optimisation in improving the efficiency of plastic waste conversion.

2.6.3 Role of Catalysts in Microwave Pyrolysis

Catalysts play a crucial role in enhancing the efficiency and selectivity of microwave pyrolysis reactions. Metals like Fe, Co, and Ni have been found to act as both microwave absorbers and catalysts, promoting the breakdown of plastics into hydrogen and carbon at lower temperatures than non-catalytic processes [2]. This dual function of catalysts in MAP is vital, as it reduces the energy required for the reaction while improving product yield and selectivity.

The catalytic performance of these metals is attributed to their ability to absorb microwave energy and convert it into heat more efficiently than conventional methods. Bimetallic catalysts, such as $\text{Ni}_3\text{Co}_2\text{O}_x$, have been shown to enhance the dehydrogenation of polyolefin plastics, producing hydrogen with high purity and significant quantities of carbon [2]. The microwave energy is absorbed by the catalyst, which in turn heats the surrounding plastic, initiating the pyrolysis process.

Additionally, the dielectric properties of catalysts play a crucial role in determining their effectiveness in MAP [40]. However, one of the challenges in this area is the limited understanding of how these dielectric properties influence the overall efficiency of the process. Further research is needed to better quantify these properties and optimise the system for industrial applications.

2.6. Application of Microwaves in Catalytic Pyrolysis of Plastics

In a novel approach, Hussain et al. demonstrated that metals can be used directly as microwave absorbers without the need for additional dielectric materials [41]. In their experiments, waste polystyrene (PS) was successfully pyrolysed using an iron mesh as an antenna to generate heat through microwave-metal interaction [41]. The iron mesh facilitated rapid heating, reaching temperatures between 1100-1200°C, resulting in the production of 80% liquid, 15% gas, and 5% char residue [41]. In a similar study, a copper coil was used as the microwave absorber, achieving temperatures of 1000-1100°C and producing 85% liquid and 10-12% gas [42]. These experiments illustrate that the shape and material properties of the metal antennas significantly influence the rate of reaction and product yield. The mechanism of heat generation in these systems is based on the repeated reflections of microwaves within the metal mesh or coil, which eventually acts as a microwave absorber due to the interaction of free electrons. This leads to volumetric heating, reaching temperatures high enough to drive the pyrolysis process [41, 42].

Although this method has shown promise, further studies are needed to optimise the control over reaction yields and product composition. These findings suggest that metals can play a more active role in microwave pyrolysis beyond traditional catalysts, by directly absorbing microwaves and enhancing heating efficiency [41].

2.6.4 Challenges and Future Directions in Microwave Pyrolysis

Despite its many advantages, MAP faces several challenges that limit its widespread adoption at the industrial level. One significant challenge is the difficulty in accurately measuring temperatures during the process. The formation of hotspots due to non-uniform heating can lead to inconsistencies in the pyrolysis reaction, making it difficult to maintain optimal operating conditions [40]. Additionally, the specific role of dielectric materials in the process remains poorly understood, particularly in how they influence the energy transfer and catalytic effects during pyrolysis [43].

Another limitation is the inability to scale up microwave pyrolysis processes effectively. While lab-scale experiments have demonstrated the feasibility of converting plastic waste into valuable products, the design of larger-scale microwave systems that can handle industrial quantities of plastic waste remains a challenge [40].

Finally, the design of microwave cavities and reactors plays a critical role in ensuring uniform heating and efficient energy transfer [44]. Recent advances in cavity design, such as the use of rotating turntables and microwave mode stirrers, have been shown to improve heating uniformity by up to 40% in some cases [45]. However, further investigations are needed to push microwave pyrolysis towards large-scale industrial applications, where cost reduction and energy efficiency are critical factors.

Despite these challenges, microwave pyrolysis remains a promising technology for plastic waste management. Continued research into catalyst design, process optimisation, and reactor development will be crucial in unlocking the full potential of this technology and bringing it closer to industrial viability [40].

2.7 Conclusion

The review of literature on MAP reveals several critical gaps that warrant further investigation. First, while the dielectric properties of certain materials like Fe, Ni, and Co are known to make them effective microwave absorbers, comprehensive studies comparing their performance in varying compositions and particle sizes are lacking. Understanding how these catalysts interact with microwave radiation, particularly under different operating conditions, could significantly enhance the efficiency of MAP processes.

Additionally, accurate temperature measurement remains a challenge, especially in environments where Electromagnetic Interference (EMI) may compromise the reliability of sensing equipment. Developing more robust and precise methods for monitoring temperature within microwave reactors is crucial for improving control over the pyrolysis process and ensuring repeatability of results.

Another notable gap lies in the comparative analysis of different microwave technologies. The literature highlights operational differences between transformer-based and inverter-based microwave systems, but the research has not yet explored how these technologies impact catalyst performance and overall efficiency in pyrolysis applications. Investigating the effects of these power delivery methods on reaction outcomes could provide valuable insights for scaling up MAP for industrial use.

In summary, the literature highlights significant opportunities to improve the understanding of MAP, particularly concerning the role of catalyst selection, accurate temperature measurement, and the efficiency of microwave technologies. These gaps are closely aligned with the challenges outlined in this study, such as ensuring reproducibility in hydrogen production and optimising catalyst performance within identified microwave hotspots. By focusing on these areas, this research aims to contribute to the development of more consistent and efficient processes for hydrogen production from plastic waste, while also advancing the broader applicability of MAP in sustainable waste management and clean energy generation.

Chapter 3

Methodology

This chapter outlines the testing methodology used to investigate the interactions between microwaves and the FeAl₂O₃ catalyst. The experimental process begins with thermal mapping to identify hotspots and cold spots within the microwave cavity, based on the distribution of electromagnetic energy. These initial tests provide critical insights into areas of constructive and destructive interference, highlighting zones with optimal electromagnetic energy concentration for microwave heating.

Subsequent experiments focus on evaluating the behaviour of the FeAl₂O₃ catalyst under controlled microwave conditions, with an emphasis on determining whether placing the catalyst and plastic mixture in a known hotspot enhances the reproducibility of hydrogen production. These tests investigate the effects of power levels and catalyst placement on the reaction, comparing results between hotspot and non-hotspot locations within the microwave cavity.

3.1 Overview of Experimental Setup

3.1.1 Microwave Models

The two microwaves used in this study are the LG NeoChef Smart Inverter Microwave and the Midea 30L Digital Microwave. Each was chosen based on its unique power delivery method and internal configuration. Their specifications are as follows:

LG NeoChef 42L Smart Inverter Microwave

The LG NeoChef (Model MS4295DIS /01) is a high-capacity inverter microwave that provides continuous power control. This continuous power mode is key to avoiding the power cycling found in traditional transformer-based microwaves, making it an ideal candidate for testing reactions under stable microwave conditions.

Midea 30L Digital Microwave (Transformer Microwave)

The Midea 30L Digital Microwave (Model EM30SILVER) operates using a traditional transformer-based power system that cycles power on and off to regulate heating. This provides a contrast to the continuous power output of the inverter microwave and was primarily used for comparison purposes.

Table 3.1: Specifications of the LG NeoChef 42L Smart Inverter Microwave

Specification	Details
Brand	LG
Model	MS4295DIS /01
Capacity	42 L
Power Output	1200 W (maximum power)
Technology	Inverter technology
Frequency	2.45 GHz
Internal Dimensions (without recess)	360 mm (W) x 365 mm (D) x 230 mm (H)
Internal Dimensions (with recess)	395 mm (W) x 406 mm (D) x 262 mm (H)

Table 3.2: Specifications of the Midea 30L Digital Microwave (Transformer Microwave)

Specification	Details
Brand	Midea
Model	EM30SILVER
Capacity	30 L
Power Output	900 W (maximum power)
Technology	Transformer-based technology with cycled power
Frequency	2.45 GHz
Internal Dimensions (without recess)	305 mm (W) x 310 mm (D) x 208 mm (H)
Internal Dimensions (with recess)	330 mm (W) x 335 mm (D) x 250 mm (H)

3.1.2 Temperature Sensing Equipment

A custom-built temperature sensing module was used to monitor temperatures during the microwave experiments. The sensing equipment was connected to a Raspberry Pi 3B+ microcontroller, which managed data collection and displayed live video and temperature readings through a web server. The camera was particularly useful in identifying potential microplasma discharges, while the temperature data was used to track heat generation during the reaction.

3.1.3 Thermal Mapping Setup

To identify areas of high electromagnetic energy concentration within the microwave cavities, thermal mapping tests were conducted using heat-sensitive thermal paper. These tests visualised the distribution of electromagnetic energy at different power levels and informed the placement of the FeAl₂O₃ catalyst for subsequent hydrogen production tests. The thermal mapping process also evaluated the effect of a custom mode stirrer on the uniformity of heating.

3.1.4 Catalyst Preparation and Testing

The FeAl₂O₃ catalyst was selected for testing based on its known catalytic properties in microwave-assisted reactions. For each test, 0.5g of FeAl₂O₃ powder was mixed with 0.5g of crushed [high-density polyethylene](#) plastic and placed in a round-bottom flask, which was purged with nitrogen gas before testing. Experiments were conducted at different power levels to evaluate the reproducibility of hydrogen production when the catalyst-plastic mixture was placed in known hotspots vs non-hotspots, as identified during thermal mapping.

3.1.5 Experimental Workflow

The following workflow was used to conduct the experiments:

1. **Thermal Mapping:** Identifying electromagnetic energy distribution within the microwave cavity, with a focus on locating hotspots.
2. **Catalyst Testing:** Investigating hydrogen production by placing the catalyst-plastic mixture in hotspots and non-hotspots at different power levels.

This structured approach ensures that the influence of microwave power settings and energy distribution on the catalytic process is thoroughly evaluated.

3.2 Sensing Module Design, Calibration, and Validation

Accurate temperature monitoring is critical to the success of this investigation, as it allows for precise evaluation of the heating behaviour of the catalysts under microwave conditions. The temperature sensing module is responsible for capturing both internal and external temperature data from the microwave cavity, ensuring comprehensive coverage across different test environments.

The temperature sensing module aimed to track temperature fluctuations during the microwave reaction, while also capturing potential microplasma discharges that could suggest the heating mechanism. The working hypothesis was that microplasma formation between the FeAl₂O₃ catalyst and plastic mixture was responsible for the observed heating effects and subsequent hydrogen production.

The following subsections describe the component selection, design of the temperature sensing module, and the calibration process, ensuring accurate temperature readings throughout the experiment.

3.2.1 Component Selection and Module Design

The decision to use thermistors and thermocouples for temperature monitoring in this investigation was driven by the cost and practicality of these components in relation to more advanced, but expensive, temperature sensing methods available for microwave heating technologies. According to Lapshinov [46], non-contact methods like spectral pyrometry and fiber-optic sensors offer high precision and are less susceptible to electromagnetic interference, but their cost and complexity render them unsuitable for the scope of this project. While fiber-optic sensors, for instance, can provide accurate measurements in high electromagnetic environments, their maximum temperature limit (300°C) and delayed response time make them impractical for rapid and high-temperature monitoring [46]. On the other hand,

3.2. Sensing Module Design, Calibration, and Validation

thermistors and thermocouples offer a balance between accuracy, cost, and ease of implementation, with thermocouples being widely used in industrial applications due to their ability to measure high temperatures up to 2000°C [46]. Despite their susceptibility to electromagnetic interference, careful shielding and placement minimise these effects, making them the most viable option for this experiment [47, 48].

Two primary temperature sensing devices are employed in the module: the DO-35 Axial Glass Case NTC Thermistor and the K-Type Stud Thermocouple, each selected for their respective strengths in monitoring external and internal temperatures.

The following outlines the components included in the monitoring, their specifications, and their intended purpose:

- **DO-35 Axial Glass Case NTC Thermistor (Model: DHT0B103J3953SY):** The thermistor has a resistance of $10\text{k}\Omega$ at 25°C and a tolerance of $\pm 5\%$. It is used to measure the temperature at various points on the exterior of the microwave cavity by placing it in drilled holes in the cavity walls. This provides external temperature readings, ensuring safe operation and monitoring of the microwave's thermal load.
- **K-Type Stud Thermocouple with Digital Converter (MAX6675):** The K-Type thermocouple is employed for high-temperature monitoring inside the microwave cavity, capable of measuring up to 700°C. The thermocouple is connected to a cold junction compensated MAX6675 digital converter for real-time temperature readings during the experiment.
- **DSJ-3808-308 USB Camera:** A camera is installed inside the microwave cavity to provide real-time video monitoring as well as record video. The camera is positioned to capture the interior of the cavity, allowing for visual inspection of the experiment in progress without needing to open the microwave door.

The temperature sensing module, including the thermistors, thermocouple, and camera, is controlled by a Raspberry Pi 3B+ microcontroller, which collects and processes temperature data and video feed. The thermistors are interfaced using the MCP3008 Analog-to-Digital Converter (ADC), while the thermocouple is interfaced through the MAX6675, ensuring accurate and reliable data acquisition.

All temperature readings and a live video feed are streamed to a web server hosted on the Raspberry Pi, enabling remote monitoring of the experiment. This setup allows for real-time observation of the temperature readings and visual verification of the catalyst behaviour without the need to open the microwave door, preventing potential disturbances to the microwave cavity's conditions. The following Figure 3.1, displays the web server setup during a thermal mapping test:

Temperature Logger and Live Camera Feed

Power Setting: Catalyst: Microwave Duration (minutes): Microwave Duration (seconds):

Recorded Data

Comments can only be added while logging is active. TR-1 to TR-8 represent the thermistors 1 to 8.

Timestamp	TR-1	TR-2	TR-3	TR-4	TR-5	TR-6	TR-7	TR-8	Thermocouple	Comment
2024-09-18 10:54:34	18.62	18.89	18.49	18.76	18.89	18.76	18.82	18.96	19.00	
2024-09-18 10:54:44	18.69	18.82	18.62	18.69	18.96	18.76	18.89	18.96	19.50	
2024-09-18 10:54:54	18.62	18.96	18.49	18.76	18.89	18.76	18.82	18.82	19.50	
2024-09-18 10:55:04	18.62	18.82	18.56	18.76	18.89	18.69	18.82	18.89	19.25	
2024-09-18 10:55:14	18.36	18.56	18.29	18.49	18.56	18.36	18.56	18.56	19.00	
2024-09-18 10:55:24	18.56	18.76	18.69	18.76	18.82	18.62	18.76	18.62	19.50	

Live Camera Feed

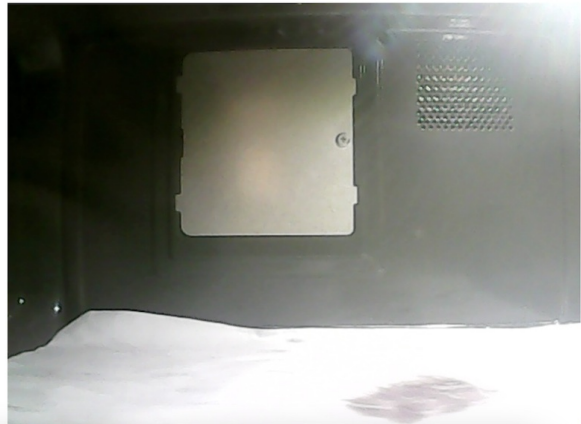


Figure 3.1: The web server displaying the thermistor, thermocouple, and camera feed in real time with time stamps.

The above figure does not display the download buttons which are present at the end of testing which allow for the temperature readings to be downloaded in a ‘.csv’ format while the video is downloaded in a ‘mp4’ format. This allows for the data processing and examination even after the tests have concluded. The code used to collect the temeperatures, control the camera, and host the webserver can be found in the github link in Appendix 8.

Camera Modifications and EMI Shielding

To mitigate the impact of [EMI](#) from the microwave cavity, the camera was modified with shielding. A metal washer covered with aluminium foil tape was used to shield the camera’s exposed circuitry, while the lens was left unobstructed to ensure clear video capture. This shielding prevents [EMI](#) from affecting the camera’s performance while ensuring that the internal components are protected from the microwaves, due to the reflective properties of aluminium.

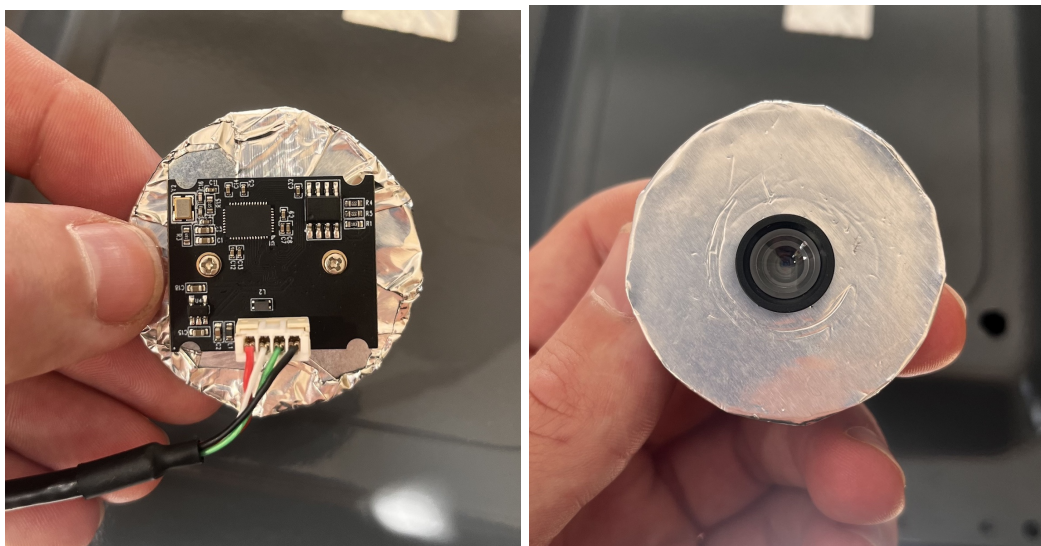
The camera was mounted onto the microwave with drilled holes in the microwave’s side wall, as shown in Figures 3.3. Care was taken to route the wiring externally to further minimise interference.

Pin Layout Description:

Below is a description of the pin layout used in the wiring schematic to connect the temperature sensing components to the Raspberry Pi.

Table 3.3 summarises the pin layout used to connect the temperature sensing components to the Raspberry Pi.

3.2. Sensing Module Design, Calibration, and Validation



(a) Rear view of the shielded camera module (b) Front view of the shielded camera module

Figure 3.2: The modified camera module for temperature monitoring, showcasing the shielding.



Figure 3.3: Camera attached to the side of the microwave allowing the lens to capture information inside while having its circuitry protected.

Table 3.3: Pin Layout for Temperature Sensing Module

Pin	Function	Description
3V3 Power Pin (Pin 1)	Power Supply	Powers the system
Ground Pins (Pin 6 and Pin 25)	Ground	Provides ground for all components
MOSI (Pin 19, GPIO10)	Data Transmission	Serial data to the MCP3008 ADC
MISO (Pin 21, GPIO9)	Data Reception	Serial data from the MAX6675 and MCP3008 ADC
SCK (Pin 23, GPIO11)	Clock Signal	Serial clock line for both the MCP3008 and MAX6675
CS (Pin 24, GPIO8)	Chip Select	Chip select for the MCP3008
CS (Pin 26, GPIO7)	Chip Select	Chip select for the MAX6675

Wiring Diagram:

Figure 3.4 provides the wiring schematic for the temperature sensing module, detailing the connections between the Raspberry Pi, the MCP3008 ADC, the MAX6675 thermocouple converter, and the thermistors.

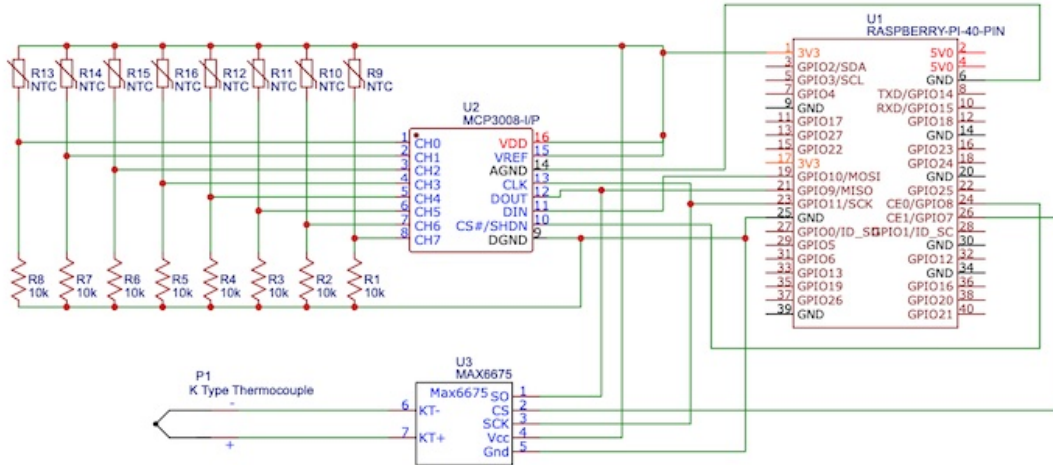


Figure 3.4: A wiring diagram illustrating the connections between the MCP3008 ADC, MAX6675 thermocouple converter, and thermistors to the GPIO pins of the Raspberry Pi for the temperature sensing module.

3.2.2 Module Calibration and Testing

To ensure accurate temperature readings from the thermistors and thermocouple, a detailed calibration process was conducted. The goal was to calibrate the thermistors against the thermocouple, which has built-in calibration via the MAX6675 digital converter, and to verify the results using an infrared thermometer.

The calibration of the **DO-35 Axial Glass Case NTC Thermistor (Model: DHT0B103J3953SY)** was carried out as follows:

- Data Collection:** Thermistor resistance was measured at three distinct temperature points: boiling water (100°C), ice water (0°C), and room temperature (approximately 18-20°C). Resistance was collected using a voltmeter, while the corresponding temperatures were measured with the K-Type Stud Thermocouple.
- Steinhart-Hart Calibration:** The resistance and temperature data were input into the online Steinhart-Hart equation calculator [49]. The temperature-resistance pairs collected and used for calibration, as well as the resulting Steinhart-Hart coefficients, are summarised in Table 3.4.

3.2. Sensing Module Design, Calibration, and Validation

Table 3.4: Steinhart-Hart Calibration Results

Measurement	Resistance (Ω)	Temperature ($^{\circ}C$)
R_1	1080000	4
R_2	14292.5	18.125
R_3	1875	69.25

The Steinhart-Hart coefficients obtained from the calibration process are shown in Table 3.5.

Table 3.5: Calibrated Steinhart-Hart Coefficients

Coefficient	Value
a	$-0.3080782548 \times 10^{-3}$
b	$4.895032621 \times 10^{-4}$
c	$-10.75680830 \times 10^{-7}$

3. **Comparison with Datasheet Coefficients:** Using the datasheet's Resistance vs Temperature curve, the resistance-temperature pairs are presented in Table 3.6.

Table 3.6: Datasheet Resistance-Temperature Pairs and Coefficients

Measurement	Resistance (Ω)	Temperature ($^{\circ}C$)
R_1	100000	-20
R_2	10000	25
R_3	1000	84

The corresponding calculated Steinhart-Hart coefficients from the datasheet are summarised in Table 3.7.

Table 3.7: Datasheet Steinhart-Hart Coefficients

Coefficient	Value
a	$1.285210645 \times 10^{-3}$
b	$2.12417456 \times 10^{-4}$
c	$1.438197044 \times 10^{-7}$

Comparing both sets of coefficients against the thermocouple readings, the datasheet coefficients resulted in temperature values averaging $1.5^{\circ}C$ below the thermocouple readings, whereas the calibrated coefficients were, on average, $1.0^{\circ}C$ higher than the thermocouple readings. Therefore, the calibrated coefficients will be used in the final system.

4. **Infrared Thermometer Validation:** To further verify the thermocouple readings, a **Non-Contact Industrial Infrared Thermometer (Model: DT8380)** was used. This device, with

a 2% accuracy between $-50^{\circ}C$ and $380^{\circ}C$, consistently matched the thermocouple's readings, validating the calibration accuracy. See Appendix 8.

5. Final Calibration: The calibrated Steinhart-Hart coefficients were implemented in the Raspberry Pi's code to convert thermistor resistance into temperature values. These values were compared to the thermocouple's readings to confirm accuracy. The calibrated thermistors now reliably monitor the microwave cavity's external surface temperature, while the thermocouple measures temperatures within the microwave cavity.

The custom-designed temperature sensing module, comprising thermistors, a thermocouple, and a USB camera, provides a robust solution for monitoring both the external and internal temperatures of the microwave cavity during the experiments. The successful calibration of the thermistors against the thermocouple, coupled with real-time video monitoring via the Raspberry Pi's web server, ensures precise and continuous data collection without disrupting the microwave environment. This system plays a critical role in accurately assessing the heating behaviour of catalysts, providing detailed thermal profiles necessary for the analysis of microwave-assisted processes.

3.2.3 Thermocouple Shielding and Arcing Mitigation

During the early stages of testing, significant challenges arose with the K-Type thermocouple due to arcing and sparking within the microwave cavity. This issue was traced to inadequate shielding of the thermocouple wires inside the wire mesh braid, leading to EMI. The exposed thermocouple wires allowed a current to be induced within the mesh, resulting in arcing, which damaged the data acquisition components, including the MCP3008 ADC.

To address this issue, multiple shielding measures were implemented based on approaches outlined in relevant literature. Van de Voort et al. [48] emphasised the importance of effective shielding for thermocouples used in microwave environments due to high levels of EMI. Based on this research, the thermocouple wires were first insulated using heat shrink tubing, which reduced direct electromagnetic exposure, but was not sufficient to fully eliminate the problem.

Further improvements were made by applying aluminum foil tape over the heat shrink tubing to create an additional layer of protection. However, additional steps were necessary to prevent arcing, as suggested by Ramaswamy et al. [47]. Drawing from their findings, a cap was crafted for the thermocouple tip using aluminum foil tape, fully enclosing the tip to further mitigate arcing. These shielding methods significantly reduced arcing inside the microwave cavity.

Despite these modifications, shield heating continued during microwave operation. As documented by Van de Voort et al. [48], this localised heating is attributed to the absorption of microwave energy by the metallic shielding material. In response to this, a commercially shielded thermocouple was purchased, which provided superior wire shielding. However, the exposed ring tip still caused some arcing.

To eliminate this issue, the cap from the original non-shielded stud thermocouple was repurposed and attached to the shielded thermocouple. This modification successfully eliminated arcing at the tip, although some heating of the braided mesh persisted. This outcome aligns with the challenges

3.2. Sensing Module Design, Calibration, and Validation

described by Van de Voort et al. [48], where fully eliminating EMI with thermocouples in microwave ovens was shown to be difficult.

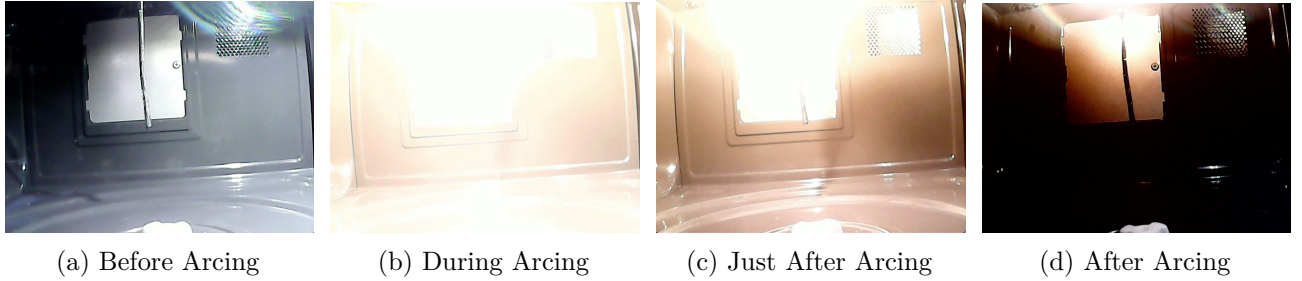


Figure 3.5: Sequence of images showing the thermocouple before, during, and after the occurrence of arcing.

The decision to modify the thermocouple's entry point into the microwave, from the top to the bottom of the cavity, was based on insights from Siddique et al. [50], who suggested that changing the thermocouple positioning can mitigate EMI and shield heating. However, during subsequent testing, shield heating remained a persistent issue even with the change in the thermocouple's entry point.

3.2.4 Commercial Shielded Thermocouple Setup

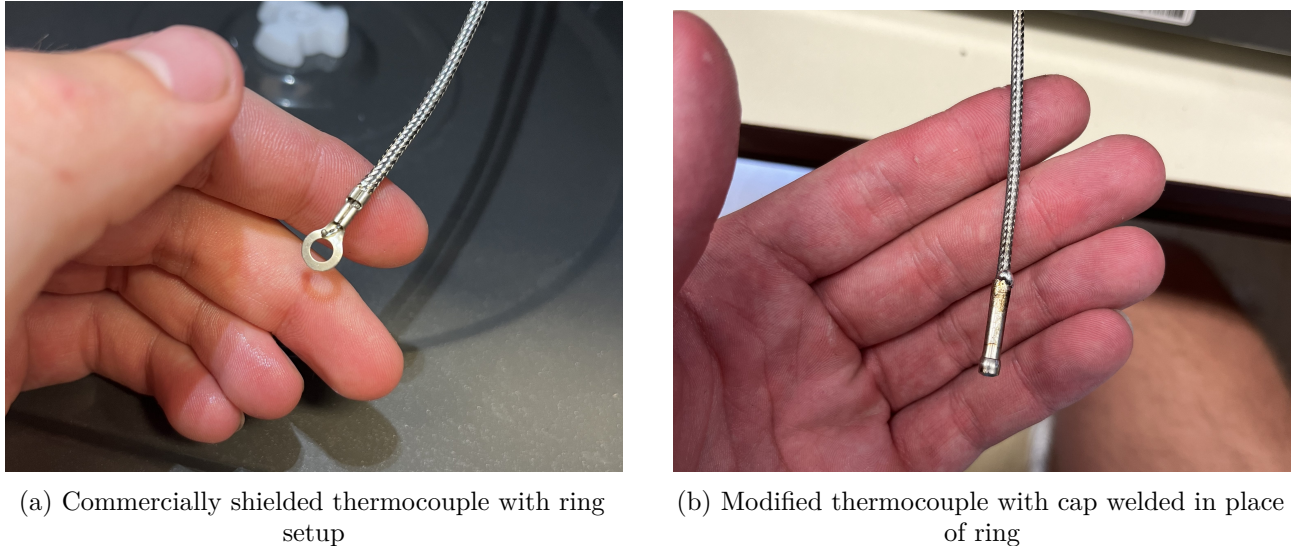


Figure 3.6: Thermocouple setup before and after the modification to reduce arcing.

The modifications mentioned above are demonstrated in Figure 3.6b. The modifications followed the recommendation by Ramaswamy et al. [47], who emphasised the importance of capping thermocouples to prevent arcing in microwave environments. The brass fitting grounded the thermocouple at the orifice in the cavity followed Van de Voort et al. [48], which stopped arcing at the entry point, but shield heating at various power levels persisted.

3.2.5 Thermistor Placement on Microwave Cavity

The thermistors were strategically positioned at various locations inside the microwave cavity to monitor temperature variations during experiments. Thermistors 1 and 2 were placed at the top front of the cavity, with thermistor 1 on the left and thermistor 2 on the right, close to the door and the magnetron. Thermistors 3 and 4 were positioned at the top back, with thermistor 3 on the left and thermistor 4 on the right. On the side walls, thermistor 5 was mounted at the back of the left-hand side of the cavity, while thermistor 6 was placed at the front of the left-hand side of the cavity. Thermistors 7 and 8 were both located at the back of the cavity, with thermistor 7 on the right and thermistor 8 on the left. These placements, as shown in Figure 3.7, were designed to provide a comprehensive temperature profile of the cavity relative to the door position.

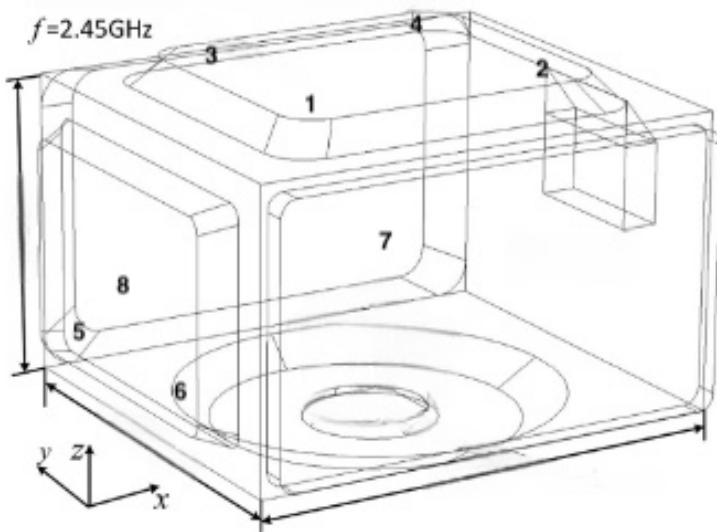


Figure 3.7: Schematic of the microwave cavity showing the placement of thermistors (labeled 1 through 8)

3.2.6 Control Experiment: Water Test

To validate the performance of the shielded thermocouple, a control experiment was conducted using water as a test medium. Water was selected due to its well-characterised thermal properties, specifically its boiling point of 100°C under standard conditions, making it an ideal medium for verifying temperature measurement accuracy. The inverter microwave was selected for this test due to its variable output power.

The experimental procedure was as follows:

- 1. Thermocouple Placement:** The thermocouple was fully submerged in 125 mL of water, contained within a round-bottom flask. Care was taken to position the thermocouple centrally to ensure even exposure to the water's heat.
- 2. Microwave Power Levels:** The microwave was operated at multiple power levels (200W, 400W, 700W, 1000W, and 1200W).

3. **Test Duration:** The test duration varied based on power level, with each test being conducted until the water began to boil.
4. **Data Collection:** The temperature was recorded using the thermocouple at 10-second intervals to observe the temperature progression until the water reached its boiling point.
5. **Safety Precautions:** Due to the shielding and potential electromagnetic interactions, tests were stopped immediately in case of arcing or abnormal behaviour.

This control experiment was essential for ensuring the thermocouple's accuracy when exposed to a high-loss material like water, which provides a stable boiling point reference. Results from this experiment will be presented in chapter 4, including temperature profiles at each power level.

3.2.7 Thermocouple Placement Tests with Metallic Powder

To assess the performance of the shielded thermocouple with metallic powders, a series of tests were conducted using FeAl₂O₃ as the metallic powder. These tests aimed to evaluate how well the thermocouple tracked temperature when in contact with or near metallic materials in a microwave heating environment, with particular focus on temperature accuracy and EMI shielding.

The experimental procedure was as follows:

1. **Thermocouple Placement:** Three scenarios were tested:
 - **Thermocouple Embedded in Metallic Powder:** The thermocouple was directly embedded within the FeAl₂O₃ powder inside a 250 mL round-bottom flask, with the aim of recording the temperature directly within the powder bed.
 - **Thermocouple Suspended Above the Powder:** The thermocouple was placed 1-2 cm above the metallic powder, without making direct contact, to observe the temperature rise due to heat radiating from the powder.
 - **Control Test Without Metallic Powder:** In the control scenario, the thermocouple was placed in the empty round-bottom flask, with no powder present, to establish a baseline performance in the absence of metallic material.
2. **Microwave Power Levels and Duration:** The inverter microwave selected for these tests as it could output 200W. For all tests, the microwave was set to operate at 200W for a duration of 1 minute and 30 seconds. This power level was selected to ensure sufficient heating while minimising the risk of arcing between the thermocouple and the metallic powder.
3. **Data Collection:** Temperature readings were captured every 2 seconds throughout each test to provide detailed insight into how the thermocouple responded in each scenario.
4. **Safety Precautions:** Due to the increased risk of arcing in the presence of metallic materials, experiments were closely monitored. The tests were immediately halted if any signs of arcing, abnormal heating, or other unsafe conditions occurred. Shield heating was also closely observed to ensure the safety of the equipment.

This experiment was essential to validate the thermocouple's performance in the challenging environment of metallic powders, which pose unique challenges due to their interaction with microwaves. Results, including temperature profiles and any observed interactions, will be presented in chapter 4.

3.3 Thermal Mapping of Microwave Cavity

To evaluate the distribution of electromagnetic energy within the microwave cavity, a thermal mapping test was conducted. Wet thermal paper was placed on a cardboard framework inside each microwave to identify areas of constructive and destructive interference during microwave operation at various power levels. The thermal paper visibly changed colour in response to the water heating, providing a visual representation of where [electromagnetic waves](#) were most concentrated, thereby creating areas of more intense heating. The terms 'hot spots' and 'cold spots' are used to represent areas where the electric field is the most intense due to [electromagnetic waves](#) being constructively interfered (hot spots) or destructively interfered (cold spots), which in turn influenced the heating patterns.

Additionally, a mode stirrer was tested to assess its effect on improving the uniformity of microwave energy distribution. Tests were conducted both with and without the mode stirrer to compare the resulting electromagnetic energy distribution patterns.

3.3.1 Preparation of Thermal Paper

The thermal paper used in this test was standard heat-sensitive paper, commonly used in receipt printers, which changes colour when exposed to heat. For the experiment, the thermal paper was cut and soaked in water, then evenly distributed on a rectangular cardboard grid. To accommodate the mode stirrer, a slit was made in both the thermal paper and the cardboard, allowing the stirrer to rotate freely without interfering with the paper. The grid's dimensions were selected based on the internal dimensions of each microwave cavity: *360mm (W) x 365mm (D)* for the inverter microwave (LG NeoChef) and *305mm (W) x 310mm (D)* for the transformer microwave (Midea). This ensured comprehensive coverage of the cavity to capture the electromagnetic distribution accurately.

3.3.2 Mode Stirrer Design and Implementation

A custom mode stirrer was designed using a wooden dowel and cardboard blades covered with aluminium foil tape. The cardboard blades were shaped into flat structures and attached to the wooden dowel. The following images display the construction of the mode stirrers:

3.3. Thermal Mapping of Microwave Cavity



(a) Top-down view of the mode stirrer.

(b) Side view of the mode stirrer.

Figure 3.8: Pictures displaying different orientations of the mode stirrers used in the experiment.

The mode stirrer was placed on the microwave's turntable motor, replacing the standard rotating plate. The stirrer was rotated by the turntable motor during the tests in an attempt to distribute the microwave energy more evenly across the cavity by reducing areas of destructive interference.



Figure 3.9: The mode stirrer's installation on the turntable motor and the camera lens.

3.3.3 Execution of the Test

Thermal mapping was performed at three power levels (1200W, 1000W, and 700W) in the inverter microwave and at a fixed power level of 900W in the transformer microwave. Each power level was tested three times, both before and after the mode stirrer was introduced. The thermal paper was observed for colour changes during microwave operation, with ‘hot spots’ (areas of constructive interference) identified by rapid colour changes, while ‘cold spots’ (areas of destructive interference) remained unchanged. Each test lasted for 60 seconds to capture early-stage heating patterns without overexposure of the thermal paper. Pictures were taken after each test, with notations indicating where the hot spots appeared within the microwave cavity.

Note: No impressions were observed on the thermal paper at lower power levels, such as 400W, despite consistent heat distribution patterns across all power levels. This suggests that even at reduced wattages, lower intensity energy is present and can still provide useful insights into the overall heat distribution, albeit with less visual impact.

3.3.4 Comparison of Results with and without Mode Stirrer

The thermal mapping tests were designed to evaluate:

1. The distribution of electromagnetic energy at different power levels (1200W, 1000W, 900W, and 700W).
2. Differences in the energy distribution between the LG NeoChef inverter microwave and the Midea transformer microwave.
3. The effect of the mode stirrer on reducing areas of destructive interference and creating a more uniform energy distribution.

3.4 Hydrogen Production Testing

The objective of this test was to determine whether placing a mixture of plastic and catalyst in known electromagnetic field ‘hotspots’ within the microwave cavity would make the experiment repeatable – hydrogen produced in every test. These ‘hotspots’ were identified during the thermal mapping tests, and the goal was to achieve reproducible results. The focus of this test was on confirming whether hydrogen was produced, rather than quantifying the amount of hydrogen produced. The LG NeoChef Smart Inverter microwave was chosen for its ability to provide continuous, variable power output, ensuring a consistent energy supply throughout the experiment. The transformer microwave was excluded from this study as it does not have variable power output and operates using power cycling, which would interfere with consistent heating.

3.4.1 Materials and Equipment

Table 3.8: Table showing the Experimental Setup and Parameters

Parameter	Description
Microwave	LG NeoChef Smart Inverter Microwave (1200W max output)
Plastic Material	0.5g of HDPE , crushed and cut into smaller pieces
Catalyst	0.5g of FeAl_2O_3 catalyst (non-reduced)
Flask	250 mL round-bottom flask
Purge Gas	Nitrogen, used to purge the flask before conducting the heat experiments
Video Recording	A phone was used to record the reaction outside of the microwave cavity to observe hydrogen bubbles
Thermistor Sensors	Used to monitor the temperature of the microwave cavity
Additional Cooling	An external fan was used to aid in cooling the microwave during extended test periods to prevent overheating

Note: One test was performed using the reduced form of the catalyst

3.4.2 Procedure

Experimental Setup

For each test, a mixture of 0.5g [HDPE](#) plastic and 0.5g of FeAl_2O_3 catalyst was placed inside a 250 mL round-bottom flask. The flask was purged with nitrogen gas before each test to ensure an inert environment, preventing any unwanted combustion.

Two primary test conditions were evaluated:

- Cold Tests:** The flask was placed in a location within the microwave cavity not identified as a hotspot.
- Hot Tests:** The flask was placed in a known hotspot identified during the thermal mapping, where [electromagnetic waves](#) constructively interfered and produced higher energy densities.

The following image depicts the experimental setup before conducting one of the hot tests, with the flask positioned in a known hotspot for optimised energy absorption.

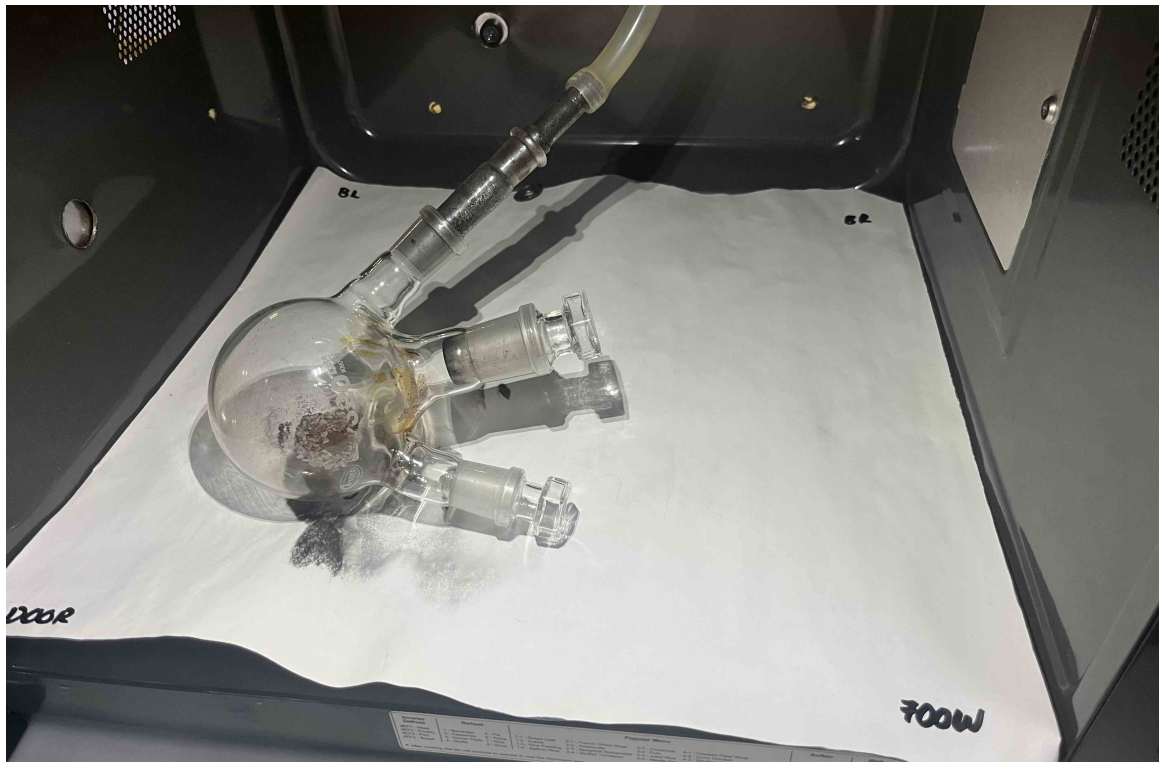


Figure 3.10: Flask positioned in a known hotspot before conducting the hot test.

Power Levels and Durations

The tests were conducted at five different power levels (200W, 400W, 700W, 1000W, and 1200W). The test durations varied according to the power level and heating concerns in the cavity. The 1200W test was excluded from the hot tests due to concerns about overheating and potential equipment failure, as the microwave had been operated for extended periods. An external fan was used to help cool the microwave after each test, though it may have affected the readings from the thermistor sensors. Each cold test was run for 5 minutes at all power levels except 1200W, which was shortened to 2 minutes 30 seconds due to overheating concerns. The hot tests were conducted for 4 minutes at all power levels, with the 1000W test shortened to 2 minutes 30 seconds due to similar heating issues.

This series of experiments aimed to establish whether placing the plastic and catalyst mixture in known hotspots within the microwave cavity would make hydrogen production repeatable under different power levels and time durations. The continuous power output of the inverter microwave provided consistent energy absorption by the catalyst, ensuring the reliability of the testing process.

3.4.3 Data Collection

For each test, the following data was collected:

Table 3.9: Data Collection and Observation Methods

Parameter	Description
Hydrogen Production	Observations were made to confirm the presence of hydrogen, indicated by bubbles appearing in the reaction flask and the plastic melting. The reaction was recorded with a phone camera outside the microwave cavity to track hydrogen production.
Temperature Data	Thermistors recorded the internal temperature of the microwave cavity throughout the tests to monitor potential overheating and assess the thermal environment.
Visual Observations	A camera inside the microwave cavity was used to confirm that the reaction proceeded without any unexpected disruptions. This camera was not used to directly observe hydrogen production.

3.5 Inverter vs Transformer Hydrogen Production Test

The objective of this test was to compare the performance of inverter-based and transformer-based microwaves in hydrogen production, specifically by evaluating their energy densities.

The microwave technologies selected for the test were as follows:

- 1. 1200W, 42L Transformer Microwave:** The LG NeoChef Smart Inverter microwave has an energy density of 28.57 W/L, calculated as 1200W divided by 42L of cavity volume.
- 2. 900W, 30L Inverter Microwave:** The Midea Digital microwave has a similar energy density of 30 W/L, calculated as 900W divided by 30L of cavity volume.

To eliminate any cycling effects in the transformer-based microwave and ensure a fair comparison of energy densities, both microwaves were operated at full power during the tests. A reduced FeAl₂O₃ catalyst was utilised.

Each test was conducted for a duration of 3 minutes. A mixture of 0.5g of HDPE plastic and 0.5g of FeAl₂O₃ catalyst was placed inside a round-bottom flask, purged with nitrogen gas to create an inert atmosphere. The flask was positioned in a known hotspot within each microwave cavity, identified during previous thermal mapping tests. The volume of hydrogen produced was measured using the displacement method in the reaction flask. The tube from the round-bottom flask, which contained the metallic powder and plastic mixture, was inserted into an inverted reaction flask filled with water. As hydrogen was produced during the reaction, it displaced the water in the flask, and the volume of displaced water was directly measured using the graduated markings on the reaction flask.

By ensuring the energy densities of the two microwave systems were comparable, the goal was to evaluate the differences in hydrogen production and overall reaction performance between the two systems under consistent energy input conditions.

Chapter 4

Results

This chapter presents the results obtained from the experiments conducted as part of the investigation into the interactions between the FeAl₂O₃ catalyst and microwaves. The results provide insights into the behaviour of microwave cavities at different power levels, the performance of the sensing module, and the reproducibility of hydrogen production in relation to catalyst placement.

4.1 Temperature Sensing Module Tests

The following sections present the results obtained from the temperature sensing module tests.

4.1.1 Control Experiment: Water Test

To ensure the reliability of the thermocouple measurements during microwave operation, a control water test was conducted in the inverter microwave. In this test, the thermocouple was used to monitor the temperature increase of water placed inside the microwave cavity. The results and observations from this test are presented below.

Observations:

The temperature rise was consistent across most power levels, with the thermocouple steadily recording the water's increase until it plateaued at around 100°C, confirming the boiling point. However, the 200W test was cut short due to fluctuating readings, which exhibited inconsistent rises and falls. Throughout the experiments, the external thermistors demonstrated stability, showing a slow, steady increase, though their readings were significantly lower than the thermocouple's, suggesting that they primarily tracked heat diffusion from the water and surrounding cavity. The time to reach boiling decreased as power levels increased, with boiling occurring more rapidly at 700W, 1000W, and 1200W. In contrast, the 200W test did not run long enough to reach boiling. Once the water reached 100°C, the thermocouple readings plateaued, indicating that the system accurately measured the boiling point and reached thermal equilibrium. Additionally, steam produced during boiling affected some thermistor readings, particularly thermistors 2, 1, and 6, as rising steam and airflow from the magnetron's fan directed heat towards those sensors. The graphs used to make these observations are presented on the following page.

4.1. Temperature Sensing Module Tests

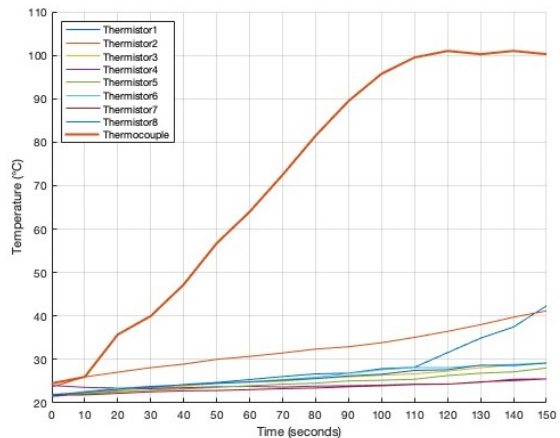
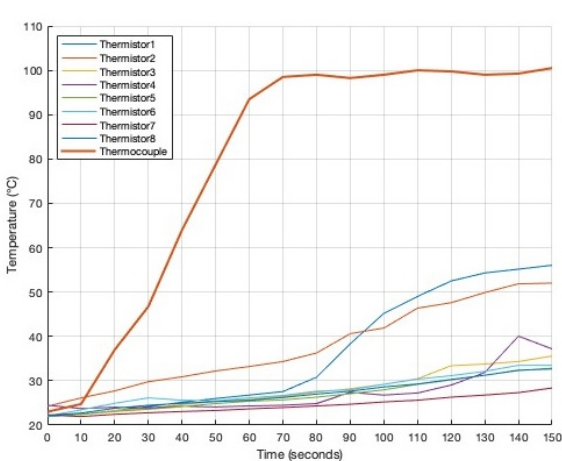
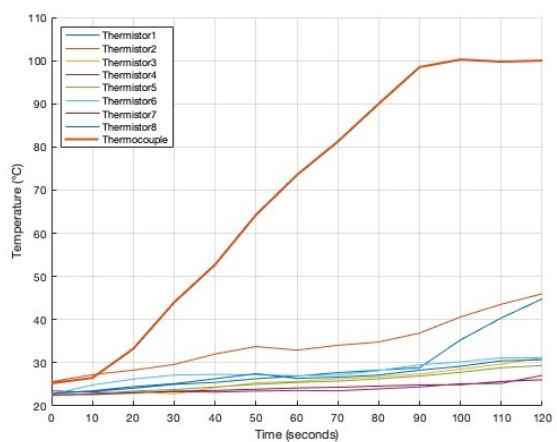
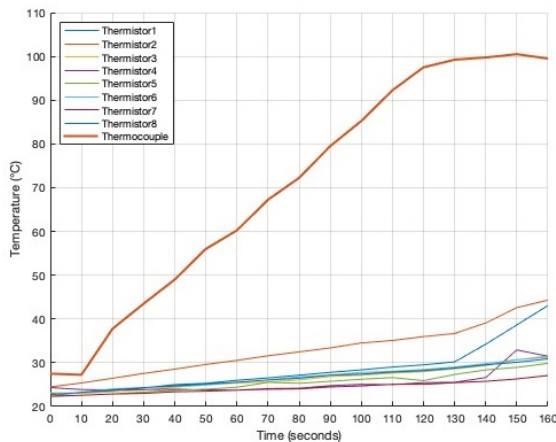
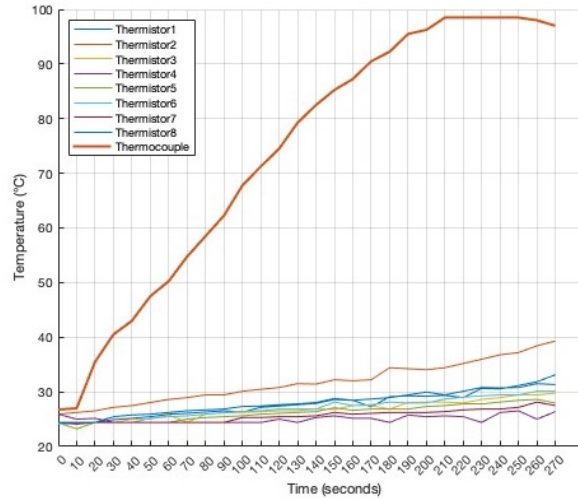
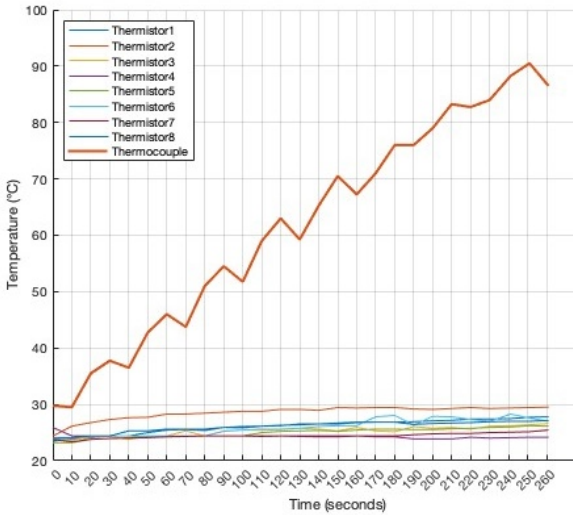
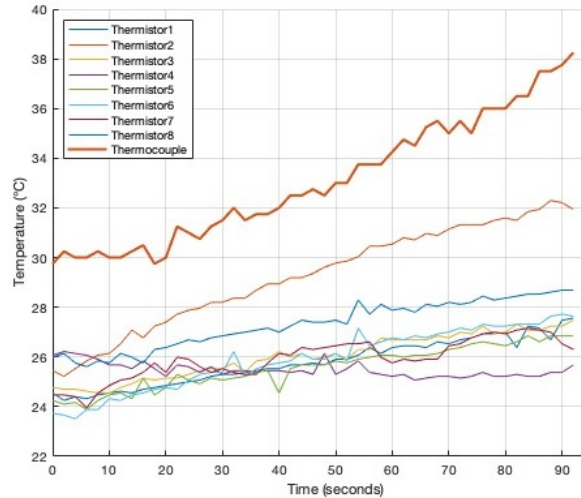


Figure 4.1: Temperature readings from water control experiments at various power levels, measured by thermocouple and thermistors.

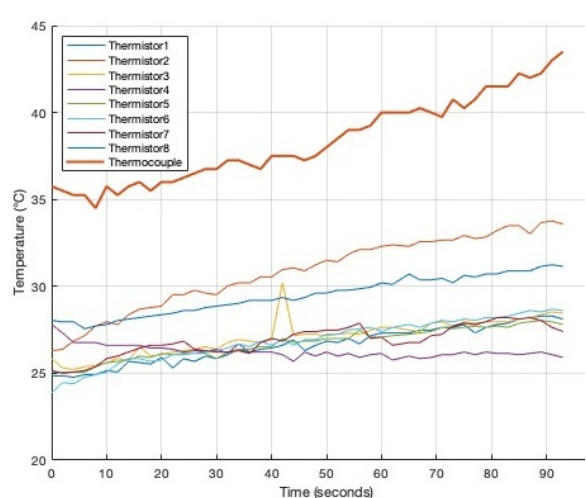
4.1.2 Thermocouple and FeAl₂O₃ Tests

Thermocouple Placed Above Powder

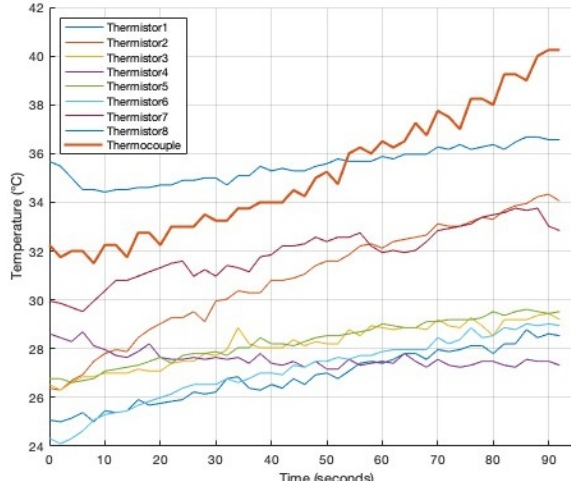
The first set of tests was conducted inside the inverter microwave with the thermocouple positioned approximately 1-2 cm above the FeAl₂O₃ catalyst. These tests aimed to observe the temperature response of the thermocouple in close proximity to the metallic powder, without direct contact. The results from this configuration are presented below.



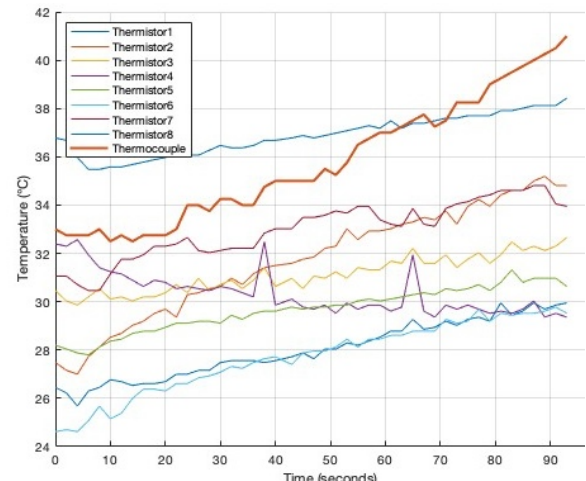
(a) Above Powder Test 1



(b) Above Powder Test 2



(c) Above Powder Test 3



(d) Above Powder Test 4

Figure 4.2: Temperature data from thermocouple and thermistors during the Above Powder tests at 200W for FeAl₂O₃ catalyst.

Observations:

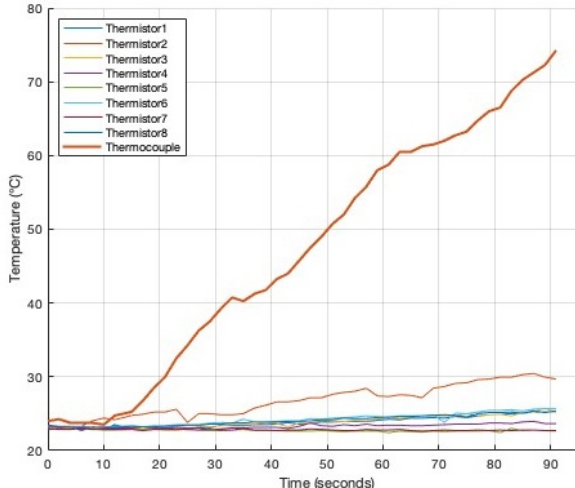
During the above powder tests, the thermocouple exhibited a steady increase in temperature, reaching approximately 40°C by the end of each test. The temperature rise was gradual and smooth, with no abrupt spikes or fluctuations, suggesting minimal EMI or arcing during the tests. The thermistors displayed relatively stable readings, ranging between 24°C and 34°C, with some minor increases observed in thermistors 1, 2, and 4, possibly indicating slight heating in specific regions of the microwave cavity.

4.1. Temperature Sensing Module Tests

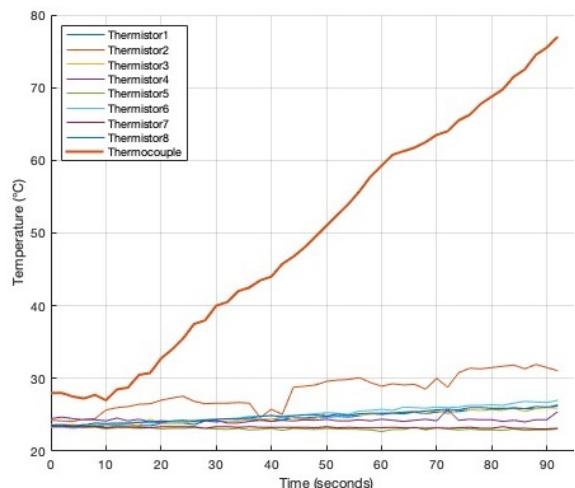
However, the temperature increase in the thermocouple remained limited, and no significant changes in the powder's heating behaviour were observed.

4.1.3 Thermocouple Placed In Powder

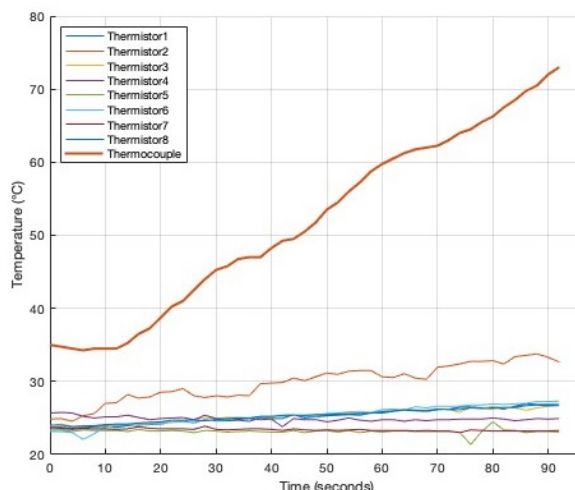
The second set of tests involved placing the thermocouple directly into the FeAl₂O₃ catalyst. This configuration allowed for the measurement of any potential direct heat transfer from the metallic powder to the thermocouple during microwave exposure. The temperature changes inside and outside of the inverter microwave recorded during this test are detailed below.



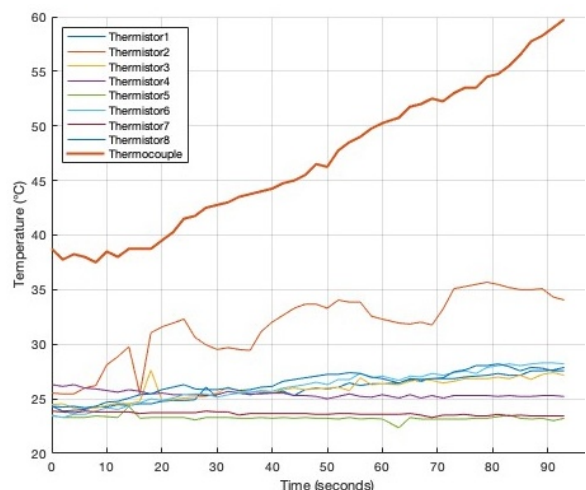
(a) In Powder Test 1 at 200W



(b) In Powder Test 2 at 200W



(c) In Powder Test 3 at 200W



(d) In Powder Test 4 at 200W

Figure 4.3: Temperature data from thermocouple placed in FeAl₂O₃ powder during 200W microwave tests.

Observations:

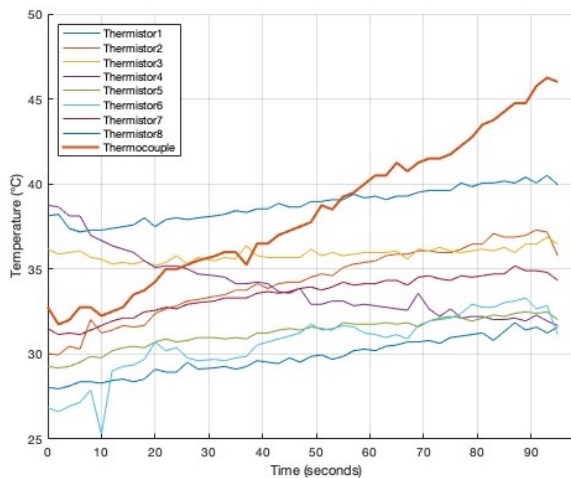
As shown in Figures 4.3a to 4.3d, the thermocouple exhibited a notable temperature increase throughout the 90-second tests, with recorded temperatures reaching upwards of 60°C to 77°C. The temperature rise was consistent across all trials, indicating a clear interaction between the microwave energy and the

4.1. Temperature Sensing Module Tests

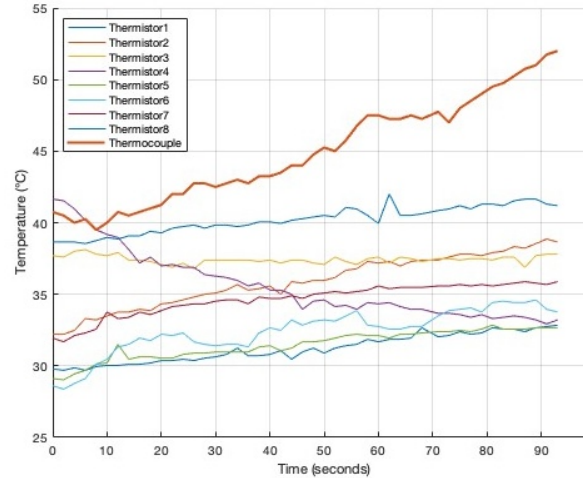
powder-thermocouple system. The thermistors, placed around the cavity, registered modest increases in temperature similar to those observed in the above powder tests, ranging between 24°C and 35°C.

4.1.4 Thermocouple Placed with No Powder Present

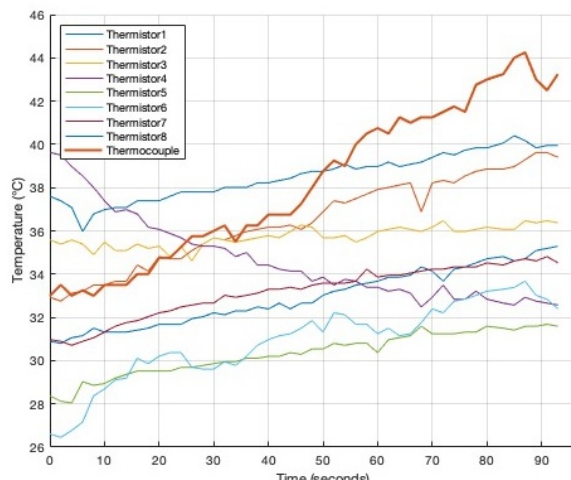
The final set of tests was conducted with the thermocouple placed inside the empty round-bottom flask, without the FeAl₂O₃ catalyst, inside the inverter microwave cavity. The results from these tests are displayed below.



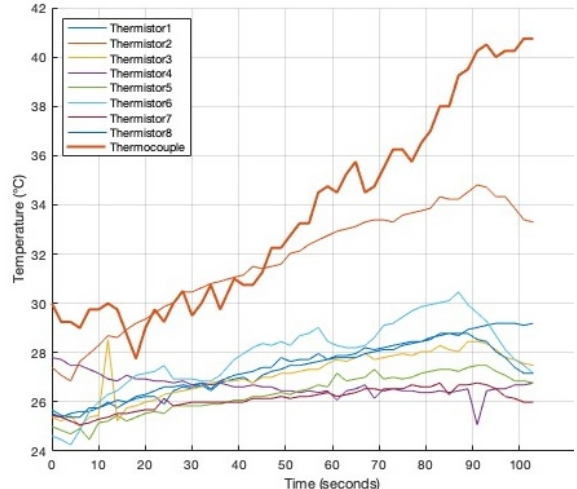
(a) No Powder Test 1



(b) No Powder Test 2



(c) No Powder Test 3



(d) No Powder Test 4

Figure 4.4: Temperature vs Time for No Powder Tests at 200W

Observations:

In the ‘No Powder’ tests, the thermocouple exhibited a steady and consistent increase in temperature, similar to the ‘Above Powder’ tests, with recorded temperatures comparable to those observed previously. No significant anomalies or abrupt spikes were detected in the thermocouple readings, indicating a gradual and uniform temperature rise throughout the test. The thermistors placed within the microwave cavity registered minimal fluctuations, suggesting that the overall temperature of the cavity remained

4.2. Thermal Mapping of Inverter Microwave

stable and relatively unaffected by the absence of the catalyst. Some minor heating was observed in thermistors 1, 2, and 3, which can be attributed to magnetron heating rather than interactions within the cavity.

4.2 Thermal Mapping of Inverter Microwave

The results from the thermal mapping tests from the inverter microwave, including comparisons with and without the mode stirrer, are presented below.

4.2.1 1200W Thermal Mapping Test



(a) Before Stirrer - Test 1



(b) Before Stirrer - Test 2



(c) Before Stirrer - Test 3



(d) After Stirrer - Test 1



(e) After Stirrer - Test 2



(f) After Stirrer - Test 3

Figure 4.5: Thermal mapping results at 1200W power level. Top row: heating patterns before the mode stirrer insertion. Bottom row: heating patterns after the mode stirrer insertion.

Hotspot Identification without Mode Stirrer

During the initial tests conducted without the mode stirrer, a prominent hotspot was observed in the front-left quadrant of the microwave cavity, closest to the door (Figures 4.5a-4.5c). This hotspot was characterised by a darkened region on the thermal paper, indicating a concentrated area of electromagnetic energy and uneven heating across the cavity. This hotspot identification was used to guide the placement of catalysts in later experiments.

Impact of Mode Stirrer

With the mode stirrer introduced, the heating patterns became more evenly distributed across the microwave cavity (Figures 4.5d-4.5f). Darkened areas appeared across multiple quadrants, suggesting that the stirrer effectively redistributed the electromagnetic energy. Although the intensity of these spots appeared slightly reduced compared to the tests without the stirrer in the latter tests, the distribution of energy was more uniform, leading to improved overall heating coverage.

4.2.2 1000W Thermal Mapping Test



(a) Before Stirrer - Test 1



(b) Before Stirrer - Test 2



(c) Before Stirrer - Test 3



(d) After Stirrer - Test 1



(e) After Stirrer - Test 2



(f) After Stirrer - Test 3

Figure 4.6: Thermal mapping results at 1000W power level. Top row: heating patterns before the mode stirrer insertion. Bottom row: heating patterns after the mode stirrer insertion.

Hotspot Identification without Mode Stirrer

At 1000W, the thermal mapping tests without the mode stirrer showed a pattern similar to that observed at 1200W, though the hotspots were smaller and slightly less defined (Figures 4.6a-4.6c). The hotspots were primarily concentrated in the front-left quadrant, but with reduced intensity due to the lower power level. These identified areas of high electromagnetic energy concentration were later used as reference points for catalyst placement in subsequent experiments.

Impact of Mode Stirrer

With the introduction of the mode stirrer, the redistribution of heat was evident but less pronounced compared to the 1200W tests (Figures 4.6d-4.6f). The darkened areas were more spread out, though the differences in heating patterns were subtler than at the higher power level. Despite this, the mode stirrer contributed to a more even distribution of electromagnetic energy across the cavity.

4.2.3 700W Thermal Mapping Test



(a) Before Stirrer - Test 1



(b) Before Stirrer - Test 2



(c) Before Stirrer - Test 3



(d) After Stirrer - Test 1



(e) After Stirrer - Test 2



(f) After Stirrer - Test 3

Figure 4.7: Thermal mapping results at 700W power level. Top row: heating patterns before the mode stirrer insertion. Bottom row: heating patterns after the mode stirrer insertion.

Hotspot Identification without Mode Stirrer

At 700W, the thermal mapping tests displayed less pronounced heating patterns compared to the higher power levels (Figures 4.7a-4.7c). The hotspots were more diffuse, with smaller and weaker darkened areas, indicating reduced energy absorption. Test 2 (4.7b) showed particularly weak results, with barely visible heating patterns compared to the other tests. Despite the lower intensity, the hotspots remained concentrated in the front-left quadrant, though they were less defined than those observed at 1000W and 1200W.

Impact of Mode Stirrer

The introduction of the mode stirrer at 700W produced a more even distribution of electromagnetic energy, though the effects were less pronounced than at higher power levels (Figures 4.7d-4.7f). While the dark spots were spread more evenly across the cavity, the heating was still concentrated in certain areas, and the overall intensity of the heating patterns remained low. These results suggest that the mode stirrer still contributed to redistributing the energy, but the impact was limited at this lower power level.

4.3 Thermal Mapping of Transformer Microwave

The results from the thermal mapping tests from the transformer microwave, including comparisons with and without the mode stirrer, are presented below.

4.3.1 900W Thermal Mapping Test

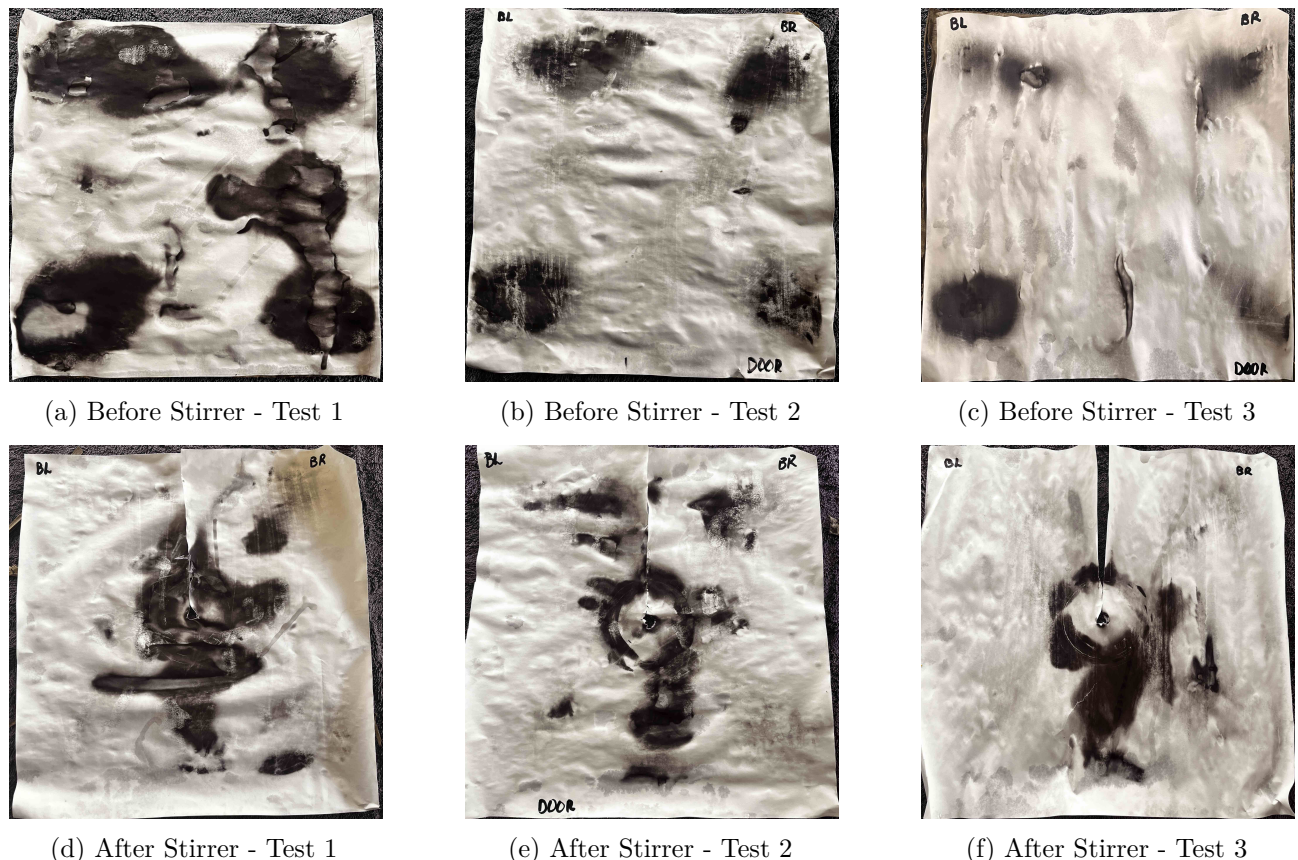


Figure 4.8: Thermal mapping results for the Transformer microwave. Top row: heating patterns before the mode stirrer was inserted. Bottom row: heating patterns after the mode stirrer insertion.

Hotspot Identification without Mode Stirrer

Without the mode stirrer, the thermal paper revealed distinct hotspots concentrated in all four corners of the microwave cavity (Figures 4.8a-4.8c). The dark spots were located in the corner quadrants, while the centre of the cavity showed minimal heating.

Impact of Mode Stirrer

After the mode stirrer was introduced (Figures 4.8d-4.8f), the heating patterns became more centralised. Although the corner heating persisted, there was a noticeable redistribution of energy towards the centre of the microwave cavity.

4.4 Hydrogen Production Testing

The results from the hydrogen production tests from the inverter microwave are presented below.

4.4.1 Test Results and Observations

Below is a summary of key test results and observations, indicating the power levels and durations of each test, followed by significant outcomes such as hydrogen production, plastic melting, and equipment issues.

Table 4.1: Summary of Hydrogen Production Tests

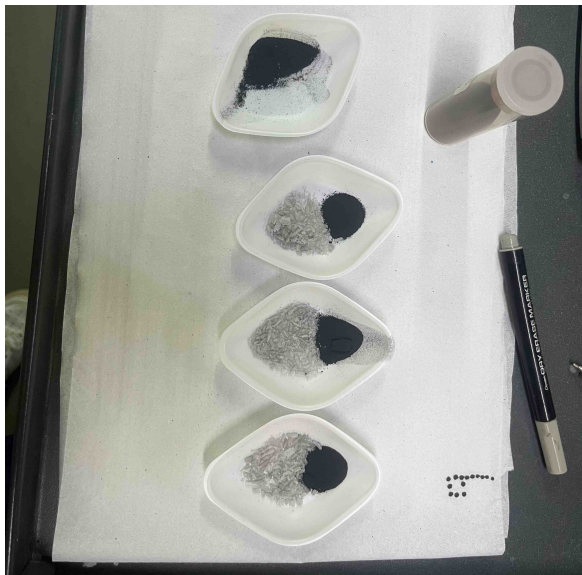
Test Condition	Power Level / Duration	Observations
Cold Test	200W / 5 minutes	No hydrogen production, plastic did not melt.
Cold Test	400W / 5 minutes	No hydrogen production, plastic did not melt.
Cold Test	700W / 5 minutes	No hydrogen production, plastic did not melt.
Cold Test	1000W / 5 minutes	No hydrogen production, microwave cavity overheated, plastic did not melt.
Cold Test	1200W / 2 minutes 30 seconds	No hydrogen production, microwave cavity overheated, test duration shortened for safety. Plastic did not melt.
Hot Test	200W / 4 minutes	Bubbles observed after 1:30 minutes, indicating hydrogen production. Plastic melted.
Hot Test	400W / 4 minutes	Hydrogen produced after 1 minute. Plastic melted.
Hot Test	700W / 4 minutes	Hydrogen production observed, but equipment issues occurred (melted glassware). Plastic melted.
Hot Test	1000W / 2 minutes 30 seconds	Hydrogen production observed, but less than previous tests due to degradation of catalyst and plastic. Plastic melted

4.4.2 Catalyst and Plastic Mixture Testing

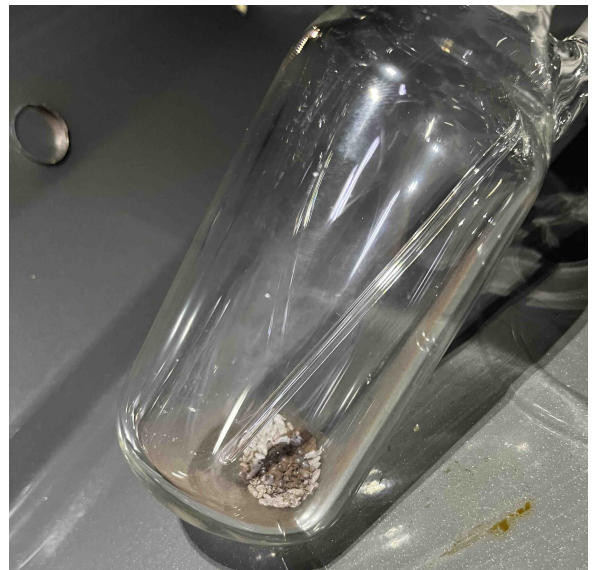
The following images provide a visual representation of the FeAl₂O₃ catalyst and HDPE plastic mixture during the hydrogen production tests. These tests aimed to observe how the catalyst and plastic mixture responded to microwave heating at various power levels. The first image shows the mixture in

4.4. Hydrogen Production Testing

its initial state before testing, while the subsequent images capture the intermediate stages of plastic melting and the final result after the reaction had taken place.



(a) Catalyst and Plastic Before Testing



(b) Plastic starting to melt during test



(c) Plastic melting observed in flask



(d) Plastic completely melted

Figure 4.9: Visuals of the catalyst and plastic during the heating stages of hydrogen production tests.

After the tests, it was evident that the plastic melted progressively as the temperature increased, leaving behind a carbon residue in the reaction flask. The metallic catalyst remained intact, although its interaction with the plastic during microwave heating was crucial in facilitating the reaction. These images highlight the physical changes the mixture underwent, offering insights into the melting process and the catalyst's behaviour under test conditions.

4.4.3 Hot Test Results: Hydrogen Detection

The plastic melted progressively as the test conditions were intensified, demonstrating the impact of heat absorption by the metallic catalyst during microwave exposure. Hydrogen production was observed during the hot tests, with the appearance of bubbles providing clear visual confirmation of the reaction. Screenshots from the video footage demonstrate the appearance of hydrogen bubbles during the hot tests. These bubbles are key indicators of successful hydrogen production.

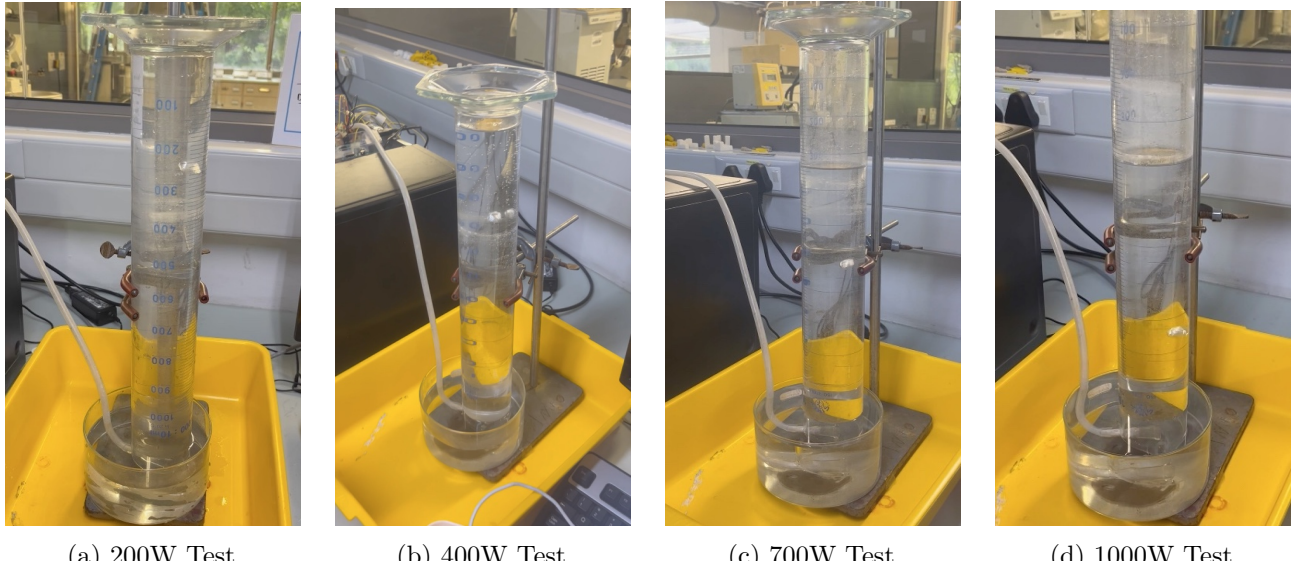


Figure 4.10: Hydrogen bubbles detected during hot tests at various power levels.

4.4.4 Overheating During 1000W Cold Test

One notable observation during the cold 1000W test was the rapid rise in temperature inside the microwave cavity, indicating overheating of the system. The following graph demonstrates the temperature profiles of various thermistors placed throughout the microwave cavity during this test.

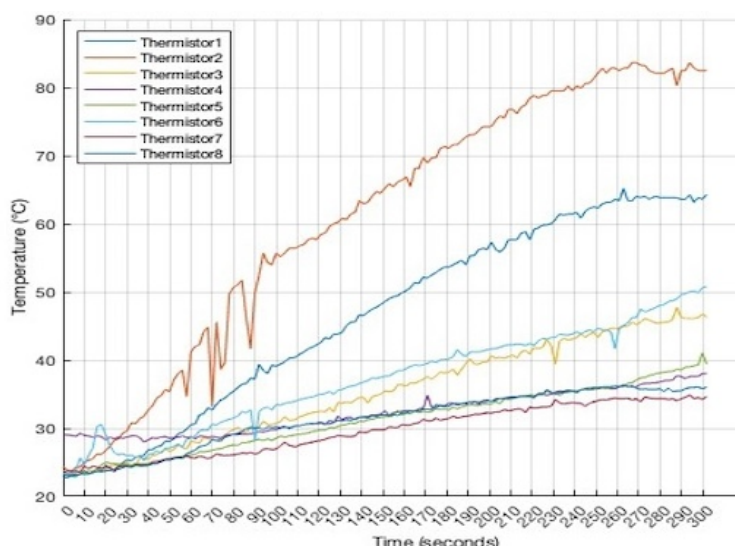


Figure 4.11: Temperature readings from the 1000W cold test showing significant overheating.

4.4.5 Glassware Melting and Interaction with Stove Putty Holder

During the hydrogen production test at 700W, a significant issue was encountered where the borosilicate glass round-bottom flask melted due to the extreme heat generated by the FeAl₂O₃ catalyst and HDPE plastic mixture. As shown in Figures 4.12a-4.12d, the glass began to deform and eventually melted completely during the reaction, compromising the integrity of the setup.



(a) Putty holder heating up.



(b) Round-bottom flask starting to deform.



(c) Flask melting during the 700W test.

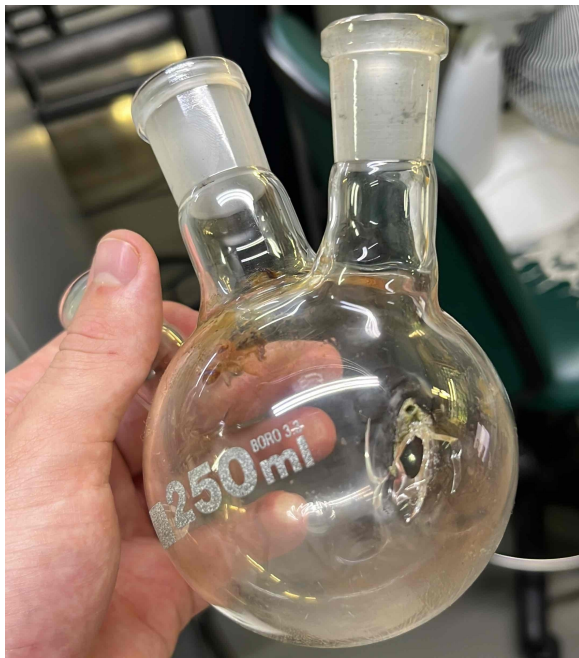


(d) Final state of the flask, completely melted.

Figure 4.12: Round-bottom flask heating during high-power tests.

In these tests, the flask was placed on a stove putty holder made of Kaylaw's fireproof stove putty (Figure 4.13) [51]. As the temperature increased, the melted glass adhered to the putty holder, causing both the glass and putty to fuse (Figure 4.13b). This fusion made it difficult to remove the glass after the test, and ultimately, the round-bottom flask was damaged beyond repair (Figure 4.13a). These results highlight the extreme temperatures reached during microwave irradiation, which exceeded the thermal limits of borosilicate glass.

4.5. Hydrogen Production: Inverter and Transformer Microwaves



(a) Broken round-bottom flask.



(b) Burnt stove putty with glass fused to it.

Figure 4.13: Post-test damage to the glass and stove putty holder.

This melting event, along with the interaction between the glass and the putty holder, is critical in understanding the limitations of the current setup when operating at high power levels for prolonged periods.

4.5 Hydrogen Production: Inverter and Transformer Microwaves

The results from the hydrogen production tests in both the inverter and transformer microwaves are presented below:

Table 4.2: Hydrogen production results from Inverter and Transformer Microwaves

Run	Microwave Type	Hydrogen Produced [mL] (Duration)
First Run	1200W Inverter Microwave	75 mL (3 minutes)
Second Run	1200W Inverter Microwave	25 mL (3 minutes)
Third Run	1200W Inverter Microwave	25 mL (3 minutes)
Fourth Run	1200W Inverter Microwave	10 mL (3 minutes)
First and Second Runs	900W Transformer Microwave	No hydrogen observed

It took approximately 30 seconds for bubbles to appear during the 1200W microwave tests, with bubble formation occurring every 3 to 4 seconds after the initial appearance. Unexpectedly, no hydrogen production was observed in the 900W microwave. No production was deduced since regardless of the length of time of operation no bubbles were observed in the reaction flask.

4.5. Hydrogen Production: Inverter and Transformer Microwaves

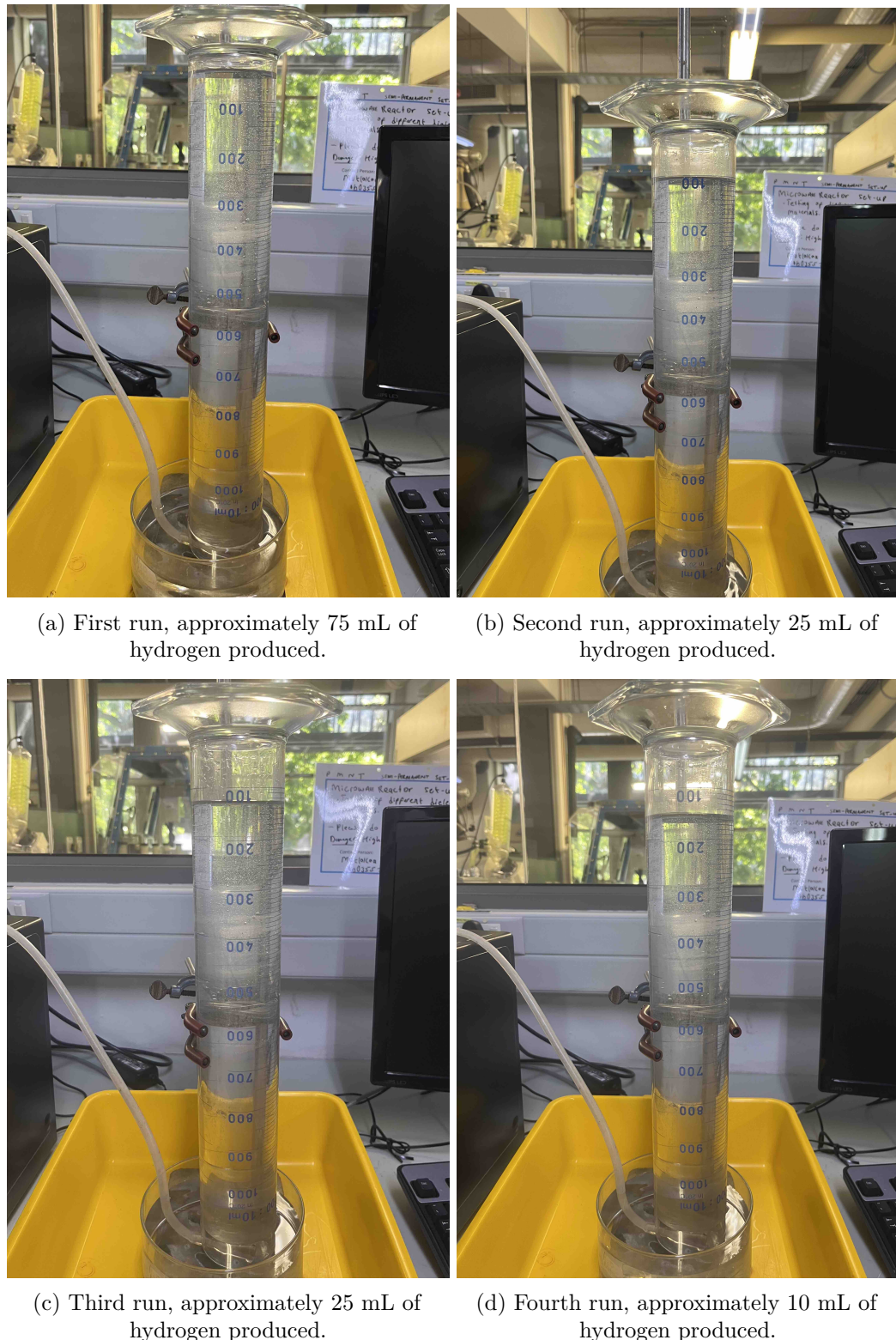


Figure 4.14: Hydrogen production results from inverter microwave runs using reduced FeAl_2O_3 catalyst.

The inverter microwave at 1200W produced measurable amounts of hydrogen during multiple runs, ranging from approximately 75 mL in the first run to 10 mL in the fourth run. The production consistently decreased over successive tests, indicating potential catalyst exhaustion. In contrast, the

900W transformer microwave, despite having a similar energy density, did not produce any detectable hydrogen in the tests conducted. The flask was placed in various positions within the microwave cavity, but no visible reaction occurred.

4.6 Summary of Key Findings

The results obtained from these experiments reveal important insights into the behaviour of microwave-assisted reactions involving the FeAl₂O₃ catalyst. The thermal mapping tests successfully identified hotspots and cold spots within the microwave cavities, which informed the placement of the catalyst for the hydrogen production tests. While the cold tests did not result in hydrogen production, the hot tests demonstrated that placing the mixture in a known hotspot significantly enhanced the reaction's reproducibility. The transformer microwave did not produce hydrogen regardless of placement in a hot spot or cold spot. The temperature measurements highlighted the challenges associated with accurately tracking the temperature of metal powders in a microwave environment. These findings will be further analysed and discussed in the following chapter.

Chapter 5

Discussion

5.1 Temperature Sensing Module Tests Discussion

5.1.1 Effectiveness of the Temperature Sensing Setup

The temperature sensing setup, consisting of the thermocouple and external thermistors, was generally effective in tracking temperature increases throughout the microwave cavity. However, the accuracy and reliability of the thermocouple measurements, particularly in the presence of catalysts, became a major concern. One of the key challenges encountered was distinguishing between actual heating of the metallic powder and [EMI](#) affecting the thermocouple probe. Shield heating emerged as a significant factor, especially in the tests where the thermocouple was placed directly in contact with the powder. This interference raises questions about the reliability of thermocouples in environments involving high electromagnetic fields and metallic powders.

Additionally, throughout the tests, no visible microplasma discharges were observed in either the recorded footage or to the naked eye. This absence does not necessarily refute the working hypothesis that microplasma formation between the FeAl₂O₃ catalyst and plastic mixture contributed to the heating mechanism. Instead, it is possible that the discharges were too small to be detected by the camera system or visible to the naked eye. A potential explanation is that the size of the metallic particles was too fine to generate sufficiently large plasma discharges that would be observable.

5.1.2 Challenges with Thermocouple Placement

During the tests where the thermocouple was placed inside the metallic powder, a significant temperature rise was recorded. However, it remains uncertain whether this temperature increase was due to the heating of the metallic powder or interactions between the thermocouple and the electromagnetic waves. In the ‘above powder’ tests, the gradual rise in temperature did not conclusively indicate whether the powder was absorbing microwave energy, or if the thermocouple was affected by shield heating. Similarly, in the ‘in powder’ tests, the sharp temperature rise suggested a potential interaction between the probe and the powder, complicating the interpretation of the results.

5.1.3 Uncertainty and Interference

The [EMI](#) introduced by the thermocouple’s metallic components further compounded the challenges of the tests. Shield heating effects suggest that the thermocouple may have absorbed microwave radiation, leading to skewed temperature readings. This uncertainty complicates the interpretation of whether the thermocouple was accurately capturing the heating of the metallic powder, or if external factors (such as [EMI](#)) played a larger role. The difficulty in isolating the true heat transfer mechanism limits the conclusions that can be drawn from these tests.

5.1.4 Impact on Understanding of Metallic Powder Behaviour

These tests offered valuable insights into the behaviour of metallic powders in microwave-assisted reactions, but the challenges with [EMI](#) and shield heating restricted their interpretive value. The inconclusive results indicate that more advanced temperature sensing methods or non-metallic thermocouples may be necessary to fully understand the microwave absorption characteristics of metallic powders.

The temperature sensing module proved to be useful in tracking general temperature changes but was insufficient for conclusively determining the heating mechanisms of the metallic powder. The challenges of [EMI](#), shield heating, and thermocouple interference underscore the need for more precise and reliable measurement techniques in future studies.

5.2 Thermal Mapping Tests Discussion

5.2.1 Effectiveness of Thermal Mapping in Identifying Hotspots

The thermal mapping tests effectively identified areas of concentrated microwave energy within the cavity. Without the mode stirrer, the tests consistently showed well-defined hotspots, typically located in the front-left quadrant of the inverter microwave and in the corners of the transformer microwave. These identified hotspots played a crucial role in guiding the placement of the catalyst-plastic mixture during the hydrogen production tests, ensuring that the mixture was placed where microwave energy was most concentrated.

5.2.2 Impact of Mode Stirrer on Heat Distribution

Introducing the mode stirrer improved the distribution of microwave energy within the cavity, as indicated by the thermal paper showing darkened areas spread across multiple quadrants. This redistribution of electromagnetic energy reduced the formation of isolated hotspots. However, the intensity of the dark spots also diminished slightly, suggesting that the mode stirrer's ability to spread energy comes at the cost of reducing the peak intensity in any single area. This trade-off between energy uniformity and concentration is important when considering applications where focused heating is required, such as in catalytic reactions.

5.2.3 Fading of Heat Patterns During Successive Tests

Over the course of successive thermal mapping tests, the heating patterns on the thermal paper showed a noticeable decline in intensity. This fading is likely due to magnetron heating during prolonged operation, which affects its efficiency in generating microwaves. As the magnetron heats up, its output may diminish, leading to less intense heating patterns. This operational factor, magnetron temperature, should be taken into account when interpreting the results of successive tests, as it may influence the consistency of microwave heating over time.

5.2.4 Differences Between Power Levels

The tests conducted at varying power levels (1200W, 1000W, 700W) demonstrated the expected behaviour of decreasing hotspot intensity with lower power. At 1200W, the thermal paper revealed

the strongest dark spots, indicating areas of concentrated microwave energy. As power decreased, the intensity and size of the hotspots diminished, with the 400W test producing no visible impression on the thermal paper, even with an extended exposure time. These findings align with the expected decrease in energy absorption at lower microwave power levels.

5.2.5 Comparison Between Inverter and Transformer Microwaves

The comparison between the inverter and transformer microwave revealed distinct differences in their heating patterns. The inverter microwave, particularly at higher power levels, displayed more concentrated hotspots, particularly without the mode stirrer. The transformer microwave, by contrast, exhibited a more distributed heating pattern, with energy concentrated in the four corners of the cavity. The introduction of the mode stirrer in both microwaves showed that while the inverter microwave benefited from a more even distribution, the transformer microwave saw a centralisation of heating, particularly in the middle of the cavity.

It's important to note that the differences in heating patterns cannot be attributed solely to the microwave technologies (inverter vs. transformer). Factors such as cavity size and shape also played a significant role in influencing the standing wave patterns, which affects how energy is distributed within the cavity. This makes direct comparison between the two systems challenging, as both microwave technology and cavity geometry contribute to the observed results.

The thermal mapping tests successfully identified critical hotspots for use in subsequent experiments and demonstrated the impact of the mode stirrer on heat distribution. However, operational factors such as magnetron temperature and power level played a significant role in the consistency of microwave heating, which must be considered in future studies. Additionally, the comparison between the inverter and transformer microwaves highlights the complexity of microwave heating, where both technology and cavity design influence the final energy distribution.

5.3 Hydrogen Production Tests Discussion

5.3.1 Impact of Hotspots on Hydrogen Production

One of the most significant findings from these tests was the clear impact of placing the catalyst and plastic mixture in identified hotspots. During the ‘cold’ tests, no hydrogen production was observed at any power level, and the plastic did not melt. This suggests that the energy absorbed in non-hotspot regions was insufficient to initiate the catalytic reaction required for hydrogen production. Conversely, in the ‘hot’ tests, hydrogen production occurred at 200W and above, with bubbles forming as a visual indicator of the reaction. The earlier onset of hydrogen production at higher power levels confirmed that placing the mixture in a hotspot improved energy absorption and accelerated the reaction.

5.3.2 Power Level and Hydrogen Production

Hydrogen production increased with higher power levels, as more energy was delivered to the reaction. However, challenges arose at higher power levels (700W and 1000W), where equipment issues, such as melted glassware, indicated that extreme conditions may damage the setup. At 1000W, hydrogen production occurred, but the rate of production was lower, likely due to catalyst and plastic degradation

after repeated tests. The 1200W test was excluded from the final dataset due to safety concerns, as the microwave showed signs of overheating, and the risk of equipment failure was high.

5.3.3 Glassware and Putty Holder Challenges

During the hydrogen production tests, one of the critical issues encountered was the failure of the glassware and the stove putty holder at high temperatures. The borosilicate glass round-bottom flask, despite its thermal resistance, melted and cracked during tests conducted at 700W, primarily due to the intense localised heating of the metallic catalyst-plastic mixture. The stove putty holder also experienced degradation, with the molten glass adhering to it. This not only halted further testing at higher power levels but also emphasised the dangers of conducting microwave-assisted reactions in high-temperature environments without adequate thermal management precautions.

The glassware failure was particularly concerning as it posed both a safety risk and a limitation on the scalability of the experiments. The putty holder degradation further underscored the necessity of selecting materials capable of withstanding the harsh conditions produced in the microwave cavity, especially during prolonged exposure at higher power levels.

These failures highlighted the importance of ensuring the robustness of the experimental setup, especially when considering tests at 1000W and 1200W power levels. Without proper thermal precautions, conducting tests at extreme temperatures would be inherently dangerous and could result in further equipment failure or safety hazards. This limitation ultimately constrained the 1200W test, as performing such an experiment without sufficient thermal protection could have led to more severe consequences. These limitations pointed to the need for more robust materials, a subject discussed further in the recommendations section.

5.4 Hydrogen Production: Inverter vs. Transformer Microwaves

The *Hydrogen Production using Inverter and Transformer Microwaves Tests* aimed to provide initial insights into the effectiveness of each system. The inverter microwave, operating at full power, successfully produced hydrogen in all four tests, though the quantity of hydrogen decreased progressively with each run.

In contrast, the transformer microwave did not produce any hydrogen during the tests, despite having a comparable energy density to the inverter microwave. This result was not unexpected given the condition of the catalyst used in the transformer microwave tests. The lack of new catalyst material available for the transformer tests meant that the same catalyst, which had already exhibited signs of degradation in the inverter tests, was used again. Subsequently, the tests for the transformer microwave could not be performed. The degradation of the catalyst is the most probable cause for the absence of hydrogen production, as opposed to any inherent issues with the transformer microwave technology itself. Other papers and experiments have demonstrated the efficacy of transformer microwaves in hydrogen production when fresh or adequately functioning catalysts are used, further reinforcing the hypothesis that catalyst exhaustion, rather than the microwave technology, was the limiting factor in this case.

5.4.1 Catalyst Exhaustion and its Implications

The results from the inverter microwave tests, in particular the decreasing hydrogen yields over time, provide clear evidence of catalyst exhaustion. This highlights the importance of catalyst regeneration or replacement strategies for maintaining consistent hydrogen production in microwave-assisted pyrolysis. The reduction in hydrogen yield in subsequent tests suggests that the catalytic sites were progressively deactivated.

Furthermore, the positioning of the reaction flask within the microwave cavity was optimised based on known microwave hotspots, yet this did not lead to hydrogen production in the transformer microwave tests. This further supports the idea that the lack of reaction was due to the condition of the catalyst, rather than the operational characteristics of the microwave itself.

5.4.2 Challenges and Limitations in Testing Setup

A major limitation of this study was the inability to produce additional fresh catalyst material in time for the transformer microwave tests. This constraint prevented a more thorough comparison between the two microwave systems. The reliance on a single batch of catalyst, which had already been partially exhausted in the inverter microwave tests, limited the conclusions that could be drawn about the relative performance of the two systems.

5.4.3 Dependence on External Factors and Unforeseen Constraints

The progress of this investigation was also impacted by external factors, particularly the reliance on the Chemical Engineering department for catalyst manufacturing. Due to the limited availability of catalysts and the time constraints involved, the study was unable to explore alternative catalysts or perform the extensive testing initially envisioned. This emphasises the importance of collaboration and planning when conducting interdisciplinary research and highlights the need for contingency strategies when external dependencies affect the research timeline.

5.5 Discussion Summary

The discussion highlighted key insights gained from the temperature sensing, thermal mapping, and hydrogen production tests. The temperature sensing setup revealed challenges with [EMI](#) and shield heating, raising questions about the reliability of thermocouples in such environments. Thermal mapping demonstrated the importance of identifying microwave hotspots for optimal catalyst placement, with the mode stirrer improving heat distribution but at the cost of peak intensity. The hydrogen production tests confirmed that placing the FeAl_2O_3 catalyst in hotspots facilitated hydrogen generation, with diminishing yields attributed to catalyst exhaustion. A comparison between inverter and transformer microwaves showed that catalyst condition, rather than microwave technology, was the likely cause for the transformer microwave's failure to produce hydrogen. These findings underline the importance of improving catalyst longevity, refining experimental setups, and addressing external dependencies to enhance future investigations into [MAP](#) for hydrogen production.

Chapter 6

Conclusions

The aim of this study was to investigate the potential of MAP for hydrogen production, with a focus on examining microplasma formation as a heating mechanism and the reproducibility of reactions when the FeAl₂O₃ catalyst is placed in identified microwave hotspots. Through the experiments, it was demonstrated that placing the catalyst in these hotspots significantly enhanced hydrogen production, particularly during the initial tests with the inverter microwave. This finding supports the hypothesis that hotspot placement plays a critical role in improving the efficiency of microwave-assisted hydrogen production.

However, a progressive decline in hydrogen yield over successive tests indicated that catalyst exhaustion was a limiting factor in the reaction's efficiency. This was further evidenced by the lack of hydrogen production in the transformer microwave tests, which likely resulted from the exhausted catalyst rather than the differences in microwave technology. These findings underscore the importance of maintaining fresh catalyst material to ensure consistent results and optimal hydrogen yields.

While the study met its key objectives, certain limitations were encountered. Equipment constraints, such as glassware failure at higher power levels, and the depletion of catalyst material restricted further exploration of some hypotheses, particularly those comparing the performance of inverter and transformer microwave technologies. The results suggest that future research should prioritise incorporating methods for catalyst regeneration, refining temperature measurement techniques, and improving the durability of materials used in high-temperature microwave reactions.

Further research is also recommended to explore the role of microplasmas as a heating mechanism in more detail. By addressing these limitations and continuing to investigate the interaction between microwaves, catalysts, and microplasmas, future studies can help enhance the efficiency and reproducibility of microwave-assisted catalytic pyrolysis for hydrogen production.

Chapter 7

Recommendations

7.1 Limitations and Challenges

Throughout the experimental process, several key limitations were identified that impacted the accuracy, consistency, and scalability of the results:

7.1.1 Limitations in Catalyst Comparison

One of the initial objectives of this study was to investigate the impact of different catalyst materials and particle sizes on the efficiency of hydrogen production in microwave-assisted pyrolysis. However, due to time constraints and external dependencies for catalyst production, we were unable to conduct a comprehensive comparison of various catalysts. The experiments primarily focused on a single FeAl_2O_3 catalyst, limiting the scope of the investigation.

7.1.2 Electromagnetic Interference and Probe Uncertainty

The main challenge encountered in the temperature sensing setup was the inability to determine whether the observed temperature increase, particularly when the thermocouple was placed inside the metallic powder, was caused by the metallic powder absorbing microwave energy and transferring that heat to the probe, or whether both the thermocouple and the powder absorbed microwave radiation and heated up together. Additionally, an interaction between the metallic powder and the thermocouple itself may have caused localised heating. Due to this uncertainty, it was impossible to confidently isolate the actual heating mechanism, rendering the results inconclusive.

7.1.3 Resistance Introduced During Soldering

Another limitation was that the resistance introduced during soldering and wiring which may have affected the accuracy of the temperature measurements, especially for the thermistors.

7.1.4 Overheating and Glassware Failure

Overheating of the microwave cavity was observed during high-power tests, which reduced the magnetron's efficiency over time. However, the melting of the borosilicate glassware during the 700W test was a separate issue caused by the extreme temperatures generated by the metallic powder and plastic combination, not due to microwave overheating. Borosilicate glass could not withstand these temperatures, leading to equipment failure.

7.1.5 Static Nature of Thermal Mapping Tests

The thermal mapping tests provided a useful visual representation of energy concentration within the microwave cavity, but were limited by their static nature. The thermal paper used in these tests

could only capture heat accumulation at specific points, failing to track dynamic changes in energy distribution during microwave operation.

7.1.6 Variability in Microwave Technologies

The comparison between the LG NeoChef Inverter Microwave and the Midea Transformer Microwave was complicated by differences in cavity size, power settings, and design. These differences made it challenging to draw definitive conclusions about the impact of microwave technology on heating behaviour, as cavity geometry also played a significant role in energy distribution.

7.2 Recommendations for Future Work

7.2.1 Temperature Module Improvements

Post-Soldering Calibration: Recalibrate the thermistors and thermocouples after soldering to account for any resistance introduced during assembly. This will ensure more accurate temperature readings during experiments.

Alternative Temperature Sensors: Investigate the use of infrared sensors or optical pyrometers, as these non-contact methods are not influenced by [EMI](#). According to B. A. Lapshinov, infrared pyrometers are effective for capturing temperature changes in microwave environments and can overcome the limitations of thermocouples in high-[EMI](#) settings [46].

Broader Calibration Range: Perform calibration across a wider range of temperatures, ensuring that the sensors maintain accuracy throughout the entire spectrum relevant to microwave-assisted reactions.

7.2.2 Microwave Cavity and Airflow Enhancements

Standardised Microwave Models: Use comparable microwave models with similar cavity sizes and power outputs to reduce variability. For example, the [Midea 20L Digital Transformer](#) [52] and [Midea 20L Digital Inverter](#) [53] models would be ideal as they are produced by the same manufacturer, both have a 20L cavity size, feature variable power outputs, and share the same maximum output power of 700W. This would allow for a more controlled investigation of the effects of microwave technology on heating behaviour.

Enhanced Cooling Systems: Install additional cooling fans or introduce improved airflow designs around the magnetron to prevent overheating during prolonged tests, especially at higher power levels.

Cooling Phases: Implement cooling phases between tests to prevent prolonged overheating and maintain microwave efficiency during long-duration experiments.

7.2.3 Thermal Mapping and Hydrogen Production Recommendations

Real-Time Energy Distribution Mapping: Implement real-time thermal mapping technologies such as infrared cameras, which can dynamically capture heat distribution within the microwave cavity

over time. Alternatively, heat-sensitive silicone pads could be used in combination with a camera to visually track how the energy distribution changes during microwave operation.

Controlled Power Settings for Hydrogen Production: Conduct hydrogen production tests at more controlled power levels, with precise monitoring of magnetron efficiency to prevent overheating. Hydrogen output should be measured and correlated with precise temperature measurements to better understand the reaction kinetics.

Improved Glassware and Containment: Replace borosilicate glass with more durable materials, such as quartz glass, which can withstand temperatures up to 1600°C. This would reduce the risk of equipment failure during high-power tests and enable longer test durations without concerns about glassware melting.

7.2.4 Catalyst Comparison and Process Optimisation

Catalyst Variety and Particle Size Testing: Comparing catalysts of varying compositions, including iron mesh catalysts and particle sizes, would have provided deeper insights into their roles in enhancing microwave absorption and catalytic performance. Future studies should prioritise these comparisons. This will help determine which catalyst composition and particle size yield the highest efficiency in MAP for hydrogen production. Additionally, using larger particle sizes may help determine whether microplasma formation is responsible for the heating mechanism, as larger particles could potentially generate observable plasma discharges. The time limitation in this study also prevented the exploration of catalyst regeneration, which is crucial for evaluating the long-term viability of MAP systems.

7.2.5 Efficiency Measurement and Energy Consumption

Power Efficiency Measurement: To accurately quantify the energy efficiency of microwave-assisted hydrogen production, future studies should attach a power meter plug to the microwave to measure the consumed power throughout the process. This will allow for the comparison of input power and output power to hydrogen yield, offering a clearer picture of the system's overall efficiency. Recording these values will help optimise the process and identify areas for energy conservation.

7.2.6 Hydrogen Production: Inverter vs. Transformer Microwaves

Catalyst Regeneration and Availability: A major limitation encountered during the transformer microwave tests was the exhaustion of the FeAl₂O₃ catalyst, which had already been used in previous inverter microwave tests. To ensure the reliability and comparability of results between different microwave technologies, it is essential to regenerate or replace catalysts between tests. Future work should focus on developing a reliable catalyst regeneration method or ensuring sufficient catalyst availability for repeated trials.

Fresh Catalyst for Comparative Studies: Comparative studies between microwave systems should be conducted using freshly prepared catalysts to avoid any discrepancies caused by catalyst degradation. This will enable a more accurate comparison between inverter and transformer microwaves, ensuring that the observed differences are due to the microwave technology rather than catalyst condition.

7.3. Summary of Key Recommendations

Improved Catalyst Longevity Testing: To extend the operational lifetime of catalysts and improve the efficiency of hydrogen production, future investigations should explore methods to prolong the catalytic activity of FeAl₂O₃ or develop more robust catalysts that can withstand prolonged microwave irradiation without losing effectiveness.

7.3 Summary of Key Recommendations

In summary, the key challenges encountered during this investigation were related to EMI, overheating of the microwave cavity, and the limitations of static thermal mapping tests. Furthermore, the exhaustion of the FeAl₂O₃ catalyst during the hydrogen production tests prevented a thorough comparison between inverter and transformer microwaves.

By addressing these challenges through improved temperature sensing technologies, more robust calibration processes, enhanced cooling systems, real-time monitoring of microwave energy distribution, and reliable catalyst regeneration methods, future experiments can build upon the findings of this study. Additionally, ensuring that fresh catalysts are used in comparative studies between microwave technologies will allow for more accurate and reliable results in the field of microwave-assisted catalytic reactions.

Bibliography

- [1] G. A. Reigstad, S. Roussanaly, J. Straus, R. Anantharaman, R. de Kler, M. Akhurst, N. Sunny, W. Goldthorpe, L. Avignon, J. Pearce, S. Flamme, G. Guidati, E. Panos, and C. Bauer, “Moving toward the low-carbon hydrogen economy: Experiences and key learnings from national case studies,” *Advances in Applied Energy*, vol. 8, p. 100108, Dec. 2022. [Online]. Available: <https://www.sciencedirect.com/science/article/pii/S2666792422000269>
- [2] J. Zhao, J. Gao, D. Wang, Y. Chen, L. Zhang, W. Ma, and S. Zhao, “Microwave-intensified catalytic upcycling of plastic waste into hydrogen and carbon nanotubes over self-dispersing bimetallic catalysts,” *Chemical Engineering Journal*, vol. 483, p. 149270, Mar. 2024. [Online]. Available: <https://linkinghub.elsevier.com/retrieve/pii/S1385894724007551>
- [3] Q. Jiang, X. Wang, Y. Zhu, D. Hui, and Y. Qiu, “Mechanical, electrical and thermal properties of aligned carbon nanotube/polyimide composites,” *Composites Part B: Engineering*, vol. 56, pp. 408–412, Jan. 2014. [Online]. Available: <https://www.sciencedirect.com/science/article/pii/S1359836813004721>
- [4] H. Talib, “Microwave-Assisted Pyrolysis and Co-Pyrolysis: Oil, Char, and Gases-A Technological Review,” *El-Cezeri*, vol. 11, no. 2, pp. 186–198, Jul. 2024, number: 2 Publisher: Tayfun UYGUNOĞLU. [Online]. Available: <https://dergipark.org.tr/en/pub/ecjse/issue/86017/1386535>
- [5] L. Ke, N. Zhou, Q. Wu, Y. Zeng, X. Tian, J. Zhang, L. Fan, R. Ruan, and Y. Wang, “Microwave catalytic pyrolysis of biomass: a review focusing on absorbents and catalysts,” *npj Materials Sustainability*, vol. 2, no. 1, pp. 1–20, Jul. 2024, publisher: Nature Publishing Group. [Online]. Available: <https://www.nature.com/articles/s44296-024-00027-7>
- [6] Y. C. Fu and B. D. Blaustein, “Pyrolysis of Coals in a Microwave Discharge,” *Industrial & Engineering Chemistry Process Design and Development*, vol. 8, no. 2, pp. 257–262, Apr. 1969, publisher: American Chemical Society. [Online]. Available: <https://doi.org/10.1021/i260030a017>
- [7] C. Ravikumar, P. Senthil Kumar, S. K. Subhashni, P. V. Tejaswini, and V. Varshini, “Microwave assisted fast pyrolysis of corn cob, corn stover, saw dust and rice straw: Experimental investigation on bio-oil yield and high heating values,” *Sustainable Materials and Technologies*, vol. 11, pp. 19–27, Apr. 2017, aDS Bibcode: 2017SusMT..11...19R. [Online]. Available: <https://ui.adsabs.harvard.edu/abs/2017SusMT..11...19R>
- [8] J. Asomaning, S. Haupt, M. Chae, and D. C. Bressler, “Recent developments in microwave-assisted thermal conversion of biomass for fuels and chemicals,” *Renewable and Sustainable Energy Reviews*, vol. 92, pp. 642–657, Sep. 2018. [Online]. Available: <https://www.sciencedirect.com/science/article/pii/S1364032118302661>
- [9] J. Kurian and G. S. V. Raghavan, “Microwave-Assisted Pyrolysis of Biomass: An Overview,” in *Production of Biofuels and Chemicals with Pyrolysis*, Z. Fang, R. L.

- Smith Jr, and L. Xu, Eds. Singapore: Springer, 2020, pp. 185–206. [Online]. Available: https://doi.org/10.1007/978-981-15-2732-6_7
- [10] S. Ethaib, R. Omar, S. M. M. Kamal, D. R. Awang Biak, and S. L. Zubaidi, “Microwave-Assisted Pyrolysis of Biomass Waste: A Mini Review,” *Processes*, vol. 8, no. 9, p. 1190, Sep. 2020, number: 9 Publisher: Multidisciplinary Digital Publishing Institute. [Online]. Available: <https://www.mdpi.com/2227-9717/8/9/1190>
- [11] X. Zhang, K. Rajagopalan, H. Lei, R. Ruan, and B. K. Sharma, “An overview of a novel concept in biomass pyrolysis: microwave irradiation,” *Sustainable Energy & Fuels*, vol. 1, no. 8, pp. 1664–1699, 2017. [Online]. Available: <https://xlink.rsc.org/?DOI=C7SE00254H>
- [12] M. Gupta and W. Wai Leong, Eugene, *Microwaves and Metals*, 1st ed. Wiley, 2007. [Online]. Available: <https://onlinelibrary.wiley.com/doi/book/10.1002/9780470822746>
- [13] A. Zaker, Z. Chen, X. Wang, and Q. Zhang, “Microwave-assisted pyrolysis of sewage sludge: A review,” *Fuel Processing Technology*, vol. 187, pp. 84–104, 2019. [Online]. Available: <https://www.sciencedirect.com/science/article/pii/S0378382018315820>
- [14] D. El Khaled, N. Novas, J. Gazquez, and F. Manzano-Agugliaro, “Microwave dielectric heating: Applications on metals processing,” *Renewable and Sustainable Energy Reviews*, vol. 82, pp. 2880–2892, 2018. [Online]. Available: <https://linkinghub.elsevier.com/retrieve/pii/S136403211731417X>
- [15] L. Ke, N. Zhou, Q. Wu, Y. Zeng, X. Tian, J. Zhang, L. Fan, R. Ruan, and Y. Wang, “Microwave catalytic pyrolysis of biomass: a review focusing on absorbents and catalysts,” *npj Materials Sustainability*, vol. 2, no. 1, pp. 1–20, 2024, publisher: Nature Publishing Group. [Online]. Available: <https://www.nature.com/articles/s44296-024-00027-7>
- [16] S. Mallakpour and Z. Rafiee, “New developments in polymer science and technology using combination of ionic liquids and microwave irradiation,” *Progress in Polymer Science*, vol. 36, no. 12, pp. 1754–1765, 2011. [Online]. Available: <https://www.sciencedirect.com/science/article/pii/S0079670011000293>
- [17] A. Borrell and M. Salvador, “Advanced Ceramic Materials Sintered by Microwave Technology,” in *Sintering Technology - Method and Application*. IntechOpen, Oct. 2018.
- [18] M. Vollmer, “Physics of the microwave oven,” *Physics Education*, vol. 39, no. 1, pp. 74–81, Jan. 2004. [Online]. Available: <https://iopscience.iop.org/article/10.1088/0031-9120/39/1/006>
- [19] J. F. Gerling, “WAVEGUIDE COMPONENTS AND CONFIGURATIONS FOR OPTIMAL PERFORMANCE IN MICROWAVE HEATING SYSTEMS,” in ‘’, 2000.
- [20] B. S. Guru and H. R. Hiziroglu, “Waveguides and cavity resonators,” in *Electromagnetic Field Theory Fundamentals*, 2nd ed. Cambridge: Cambridge University Press, 2004, pp. 502–546. [Online]. Available: <https://www.cambridge.org/core/books/electromagnetic-field-theory-fundamentals/waveguides-and-cavity-resonators/05C4434644A1C1A38992079C865667FD>
- [21] “Rectangular Waveguide in Microwave Engineering,” Aug. 2024, section: ECE. [Online]. Available: <https://graduateinsights.in/rectangular-waveguide-in-microwave-engineering/>

- [22] V. Kumar and D. K. Gupta, "Chapter 2 - Microwave components and devices for RADAR systems," in *Radar Remote Sensing*, ser. Earth Observation, P. K. Srivastava, D. K. Gupta, T. Islam, D. Han, and R. Prasad, Eds. Elsevier, Jan. 2022, pp. 29–48. [Online]. Available: <https://www.sciencedirect.com/science/article/pii/B9780128234570000124>
- [23] Dolph, "What are the standard microwave waveguides," Apr. 2024. [Online]. Available: <https://www.dolphmicrowave.com/default/what-are-the-standard-microwave-waveguides/>
- [24] S. Balaji, "Waveguides," in *Electromagnetics Made Easy*, S. Balaji, Ed. Singapore: Springer, 2020, pp. 581–617. [Online]. Available: https://doi.org/10.1007/978-981-15-2658-9_9
- [25] S. Taghian Dinani, M. Hasić, M. Auer, and U. Kulozik, "Assessment of uniformity of microwave-based heating profiles generated by solid-state and magnetron systems using various shapes of test samples," *Food and Bioproducts Processing*, vol. 124, pp. 121–130, Nov. 2020. [Online]. Available: <https://linkinghub.elsevier.com/retrieve/pii/S096030852030506X>
- [26] V. Prakasam and P. Sandeep, "Mode patterns in rectangular waveguide," *Published in International Journal of Trend in Research and Development (IJTRD)*, ISSN, pp. 2394–9333, 2017. [Online]. Available: <https://scholar.google.com/scholar?cluster=586334783577296636&hl=en&oi=scholarr>
- [27] R. R. Mishra and A. K. Sharma, "Microwave–material interaction phenomena: Heating mechanisms, challenges and opportunities in material processing," *Composites Part A: Applied Science and Manufacturing*, vol. 81, pp. 78–97, Feb. 2016. [Online]. Available: <https://linkinghub.elsevier.com/retrieve/pii/S1359835X15003917>
- [28] N. R. Council, *Microwave Processing of Materials*. Washington, D.C.: National Academies Press, Jan. 1994. [Online]. Available: <http://www.nap.edu/catalog/2266>
- [29] J. Sun, W. Wang, and Q. Yue, "Review on microwave-matter interaction fundamentals and efficient microwave-associated heating strategies," *Materials*, vol. 9, no. 4, p. 231, 2016, number: 4 Publisher: Multidisciplinary Digital Publishing Institute. [Online]. Available: <https://www.mdpi.com/1996-1944/9/4/231>
- [30] F. Hossain, J. V. Turner, R. Wilson, L. Chen, G. de Looze, S. W. Kingman, C. Dodds, and G. Dimitrakis, "State-of-the-art in microwave processing of metals, metal powders and alloys," *Renewable and Sustainable Energy Reviews*, vol. 202, p. 114650, 2024. [Online]. Available: <https://www.sciencedirect.com/science/article/pii/S1364032124003769>
- [31] J. Sun, W. Wang, Q. Yue, C. Ma, J. Zhang, X. Zhao, and Z. Song, "Review on microwave–metal discharges and their applications in energy and industrial processes," *Applied Energy*, vol. 175, pp. 141–157, 2016. [Online]. Available: <https://www.sciencedirect.com/science/article/pii/S0306261916305529>
- [32] J. Cheng, R. Roy, and D. Agrawal, "Experimental proof of major role of magnetic field losses in microwave heating of metal and metallic composites," *Journal of Materials Science Letters*, vol. 20, no. 17, pp. 1561–1563, 2001. [Online]. Available: <https://doi.org/10.1023/A:1017900214477>

- [33] ——, “Radically different effects on materials by separated microwave electric and magnetic fields,” *Materials Research Innovations*, vol. 5, no. 3, pp. 170–177, 2001, publisher: Taylor & Francis _eprint: <https://doi.org/10.1007/s10019-002-8642-6> [Online]. Available: <https://doi.org/10.1007/s10019-002-8642-6>
- [34] O. Yaln, “Ferromagnetic resonance,” in *Ferromagnetic Resonance - Theory and Applications*, O. Yaln, Ed. InTech, 2013. [Online]. Available: <http://www.intechopen.com/books/ferromagnetic-resonance-theory-and-applications/ferromagnetic-resonance>
- [35] K. H. J. Buschow, *Handbook of Magnetic Materials*. Elsevier, 2003, google-Books-ID: oC04EZ47Ex8C.
- [36] D. El Khaled, N. Novas, J. A. Gazquez, and F. Manzano-Agugliaro, “Microwave dielectric heating: Applications on metals processing,” *Renewable and Sustainable Energy Reviews*, vol. 82, pp. 2880–2892, Feb. 2018. [Online]. Available: <https://www.sciencedirect.com/science/article/pii/S136403211731417X>
- [37] F. Chen, A. D. Warning, A. K. Datta, and X. Chen, “Thawing in a microwave cavity: Comprehensive understanding of inverter and cycled heating,” *Journal of Food Engineering*, vol. 180, pp. 87–100, Jul. 2016. [Online]. Available: <https://linkinghub.elsevier.com/retrieve/pii/S0260877416300395>
- [38] “30 Years of Inverter Technology - Panasonic Canada.” [Online]. Available: <https://www.panasonic.com/ca/consumer/home-appliances-learn/panasonickitchen/30yearsofinverter.html>
- [39] H. Yang and S. Gunasekaran, “Temperature Profiles in a Cylindrical Model Food During Pulsed Microwave Heating,” *Journal of Food Science*, vol. 66, no. 7, pp. 998–1004, Sep. 2001. [Online]. Available: <https://ift.onlinelibrary.wiley.com/doi/10.1111/j.1365-2621.2001.tb08225.x>
- [40] H. Arshad, S. A. Sulaiman, Z. Hussain, Y. Naz, and F. Basrawi, “Microwave assisted pyrolysis of plastic waste for production of fuels: a review,” *MATEC Web of Conferences*, vol. 131, p. 02005, 2017, publisher: EDP Sciences. [Online]. Available: https://www.matec-conferences.org/articles/matecconf/abs/2017/45/matecconf_ses2017_02005/matecconf_ses2017_02005.html
- [41] Z. Hussain, K. M. Khan, and K. Hussain, “Microwave–metal interaction pyrolysis of polystyrene,” *Journal of Analytical and Applied Pyrolysis*, vol. 89, no. 1, pp. 39–43, Sep. 2010. [Online]. Available: <https://linkinghub.elsevier.com/retrieve/pii/S016523701000077X>
- [42] Z. Hussain, K. M. Khan, K. Hussain, and S. Perveen, “Microwave-metal Interaction Pyrolysis of Waste Polystyrene in a Copper Coil Reactor,” *Energy Sources, Part A: Recovery, Utilization, and Environmental Effects*, vol. 36, no. 18, pp. 1982–1989, Sep. 2014. [Online]. Available: <https://doi.org/10.1080/15567036.2011.557692>
- [43] S. D. Anuar Sharuddin, F. Abnisa, W. M. A. Wan Daud, and M. K. Aroua, “A review on pyrolysis of plastic wastes,” *Energy Conversion and Management*, vol. 115, pp. 308–326, May 2016. [Online]. Available: <https://linkinghub.elsevier.com/retrieve/pii/S0196890416300619>

- [44] D. Jones, T. Lelyveld, S. Mavrofidis, S. Kingman, and N. Miles, “Microwave heating applications in environmental engineering—a review,” *Resources, Conservation and Recycling*, vol. 34, no. 2, pp. 75–90, Jan. 2002. [Online]. Available: <https://linkinghub.elsevier.com/retrieve/pii/S092134490100088X>
- [45] R. Yang, Q. Chen, and J. Chen, “Comparison of heating performance between inverter and cycled microwave heating of foods using a coupled multiphysics-kinetic model,” *Journal of Microwave Power and Electromagnetic Energy*, vol. 55, no. 1, pp. 45–65, Jan. 2021, publisher: Taylor & Francis _eprint: <https://doi.org/10.1080/08327823.2021.1877244>. [Online]. Available: <https://doi.org/10.1080/08327823.2021.1877244>
- [46] B. A. Lapshinov, “Temperature Measurement Methods in Microwave Heating Technologies,” *Measurement Techniques*, vol. 64, no. 6, pp. 453–462, Sep. 2021. [Online]. Available: <https://link.springer.com/10.1007/s11018-021-01954-w>
- [47] H. Ramaswamy, J. Rauber, V. Raghavan, and F. van de Voort, “(132) Ramaswamy, H.S., Rauber, J.M., Raghavan, G.S.V. and van de Voort, F.R. (1998). Evaluation of shielded thermocouples for measuring temperature of foods in a microwave oven. J. Food Sci. Technol 35 (4) 1998.” *Journal of Food Science and Technology -Mysore-*, vol. 35, pp. 325–329, Jul. 1998.
- [48] F. R. van de Voort, M. Laureano, J. P. Smith, and G. S. V. Raghavan, “A Practical Thermocouple for Temperature Measurement in Microwave Ovens1,” *Canadian Institute of Food Science and Technology Journal*, vol. 20, no. 4, pp. 279–284, Oct. 1987. [Online]. Available: <https://www.sciencedirect.com/science/article/pii/S0315546387712000>
- [49] “SRS Thermistor Calculator.” [Online]. Available: <https://www.thinksrs.com/downloads/programs/therm%20calc/ntccalibrator/ntccalculator.html>
- [50] I. J. Siddique and A. A. Salema, “Unraveling the metallic thermocouple effects during microwave heating of biomass,” *Energy*, vol. 267, p. 126529, Mar. 2023, publisher: Elsevier BV. [Online]. Available: <https://linkinghub.elsevier.com/retrieve/pii/S0360544222034168>
- [51] “STOVE PUTTY 800G KAYLAW - FIRE PROOF.” [Online]. Available: <https://www.fowkes.co.za/product/stove-putty-800g-kaylaw-fire-proof>
- [52] Midea, “20L Digital Microwave – Midea.” [Online]. Available: <https://retail.mideasouthafrica.com/product/small-appliances/microwaves/20l-digital-microwave/>
- [53] ——, “20L Digital Inverter Microwave Silver – Midea.” [Online]. Available: <https://retail.mideasouthafrica.com/product/small-appliances/microwaves/20l-digital-inverter-microwave-silver/>

Chapter 8

Appendix A

8.1 Graduate Attribute (GA) Table

The table below outlines how the graduate attributes (GA) required for the course have been addressed in this report, along with the relevant sections where evidence can be found.

GA	Requirement	Justification and section in the report
1	Problem-solving	Identifying and defining key challenges in microwave-assisted pyrolysis and hydrogen production, proposing solutions, and testing hypotheses. Evidence in 2 , 3 , and 4 .
4	Investigations, experiments and data analysis	Detailed experimental setup, data analysis, and interpretation. Evidence in 4 and 5 .
5	Use of engineering tools	Application of MATLAB for data analysis, Jet-brains IDE PyCharm for coding and debugging, use of GitHub for version control, and microwave reactor for experiments. Evidence in 4 and 3 .
6	Professional and technical communication (Long report)	Structured writing of report, use of technical terms, and ensuring clarity in the presentation of experimental results and discussion. Evidence throughout the report, especially in the 1 , 4 , and 5 sections.
8	Individual work	Managing all aspects of the project independently, from planning to execution. Evidence in entire project report and Appendix.
9	Independent learning ability	Reviewing literature, learning new experimental techniques, and conducting independent research. Evidence in 2 and 3 sections.

8.2 Use of AI in Report Writing

AI tools were used to assist in generating structured text, helping with code debugging, and refining specific sections of this report. These tools were mainly used for:

- 1. Grammar and Clarity:** AI was used to improve sentence structure and clarify technical explanations throughout the report.

2. **Formatting and LaTeX Assistance:** AI provided support in the arrangement of LaTeX code for figures, tables, and document formatting.
3. **Code Debugging and Suggestions:** AI suggested ways to improve the code and outlined the issues which were causing the code to fail.

The content generated by AI was reviewed and modified to ensure accuracy, consistency, and adherence to the specific project goals.

8.3 Use of AI in Report Writing

AI tools were used to assist in generating structured text, helping with code debugging, and refining specific sections of this report. These tools were mainly used for:

1. **Grammar and Clarity:** AI was used to improve sentence structure and clarify technical explanations throughout the report.
2. **Formatting and LaTeX Assistance:** AI provided support in the arrangement of LaTeX code for figures, tables, and document formatting.
3. **Code Debugging and Suggestions:** AI suggested ways to improve the code and outlined the issues which were causing the code to fail.

The content generated by AI was reviewed and modified to ensure accuracy, consistency, and adherence to the specific project goals. Below are examples of how AI was used in this project:

How does this sound for the linking between methodology and results?

"The results of all the tests mentioned above are presented in the following chapter, where observations and notes will also be outlined."

That sentence provides a good transition but could be made clearer and more fluid. Here's a refined version:

"The following chapter presents the results of the tests outlined above, along with detailed observations and key findings from each experiment."

This version improves clarity and ensures the reader knows that both results and observations are covered in the next chapter.



Figure 8.1: Example of AI providing assistance with clarity and grammar improvements.

How do I decrease the space between the numbering of a chapter such as "Chapter 1" and the name of that chapter such as "Introduction"? Would I have to include something inside of my main.tex file?

Yes, to adjust the spacing between the "Chapter X" and the chapter title in a LaTeX document, you will need to modify the chapter heading style. You can do this by adding a few lines of code to your `main.tex` or `ChapterStyle.tex` file, depending on where your chapter formatting is defined.

Here's a step-by-step approach:

1. If you are using the `titlesec` package for formatting, you can control the spacing like this:

latex

 Copy code

```
\usepackage{titlesec}\titlespacing*\{\\chapter\}{0pt}{-20pt}{20pt}
```

- The first argument `{0pt}` sets the left margin (spacing from the left).
- The second argument `{-20pt}` adjusts the space before the chapter heading. A negative value reduces the space between the "Chapter X" and the chapter title.
- The third argument `{20pt}` controls the space after the title (space between the chapter title and the following text).

Figure 8.2: Example of AI assisting with LaTeX formatting for a chapter title and spacing issues.

The screenshot shows a GitHub repository interface with an AI integration. At the top, there's a status bar with a profile icon, the number '2', and a '2/2' indicator. Below this is a dark-themed code editor area.

```

I made the new log_sensors.py and got the following:
(venv) admin@microwave:~ $ python3 app.py
/home/admin/log_sensors.py:15: RuntimeWarning: This channel is
already in use, continuing anyway. Use GPIO.setwarnings(False) to
disable warnings.
    GPIO.setup(self.cs_pin, GPIO.OUT)
    * Serving Flask app 'app'
    * Debug mode: off
    Address already in use
    Port 5000 is in use by another program. Either identify and stop that
    program, or start the server with a different port.

I had to abandon the last program because it wouldn't stop so I used
^Z to stop it, should I reboot and start again since we now fixed the
stop issue and this should resolve the above issue? The script will
now also run the GPIO.cleanup()

```

< 2/2 >

Below the code editor, there's a text box containing a note about rebooting:

Yes, rebooting the system would be a good idea in this case, especially since the previous program didn't terminate properly and the Flask server is still holding onto the port. Rebooting will ensure that:

1. All previous processes, including the one running on port 5000, are stopped properly.
2. GPIO pins will be released and reinitialized correctly upon the next script run.

After rebooting, the updated script should handle the GPIO cleanup and stop the logging properly using the new `stop_logging()` function, so you shouldn't encounter the same issue again.

Steps:

1. **Reboot the system:** This will clear any running processes and GPIO issues.
2. **Run your `app.py` after rebooting:** This should work smoothly now with the correct port and GPIO handling.

Let me know how it goes after rebooting!

Figure 8.3: Example of AI providing suggestions and debugging help for code used in the project.

8.4 GitHub Repositories

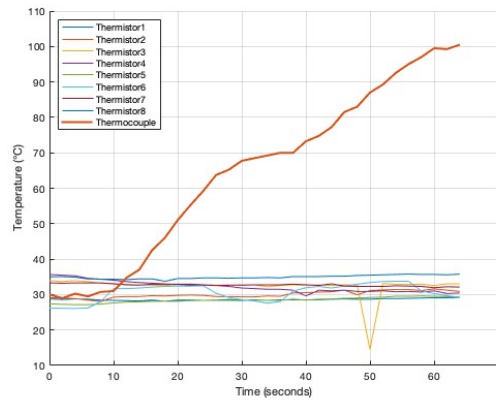
The code used for the project is hosted in two separate repositories to maintain clarity and organisation. Links to the repositories are provided below:

- **Code Repository:** The primary code used for data processing, simulations, and control systems is available at the following link: https://github.com/CaideSpries/mw_service
- **Project Files and Documentation Repository:** Additional materials such as project documents, experimental setups, schematics, and report files will be available in a separate repository: https://github.com/CaideSpries/mw_project_docs

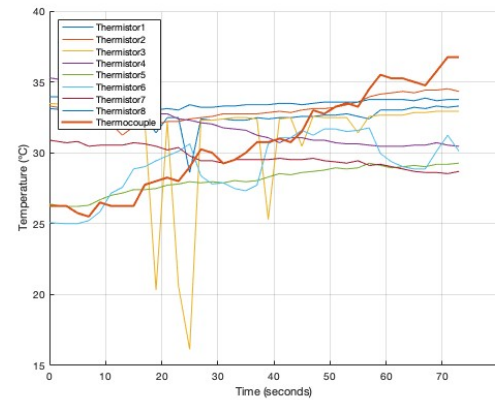
8.5 Sensing Module Calibration and Validation Pictures

8.5.1 Thermocouple at the Bottom of the Cavity

The thermocouple was first placed at the bottom of the cavity for temperature readings during the microwave-assisted catalytic pyrolysis process. The following figures show the temperature readings as recorded by the thermocouple and thermistors at various power levels.



(a) Temperature profile at 1 minute 0 seconds.

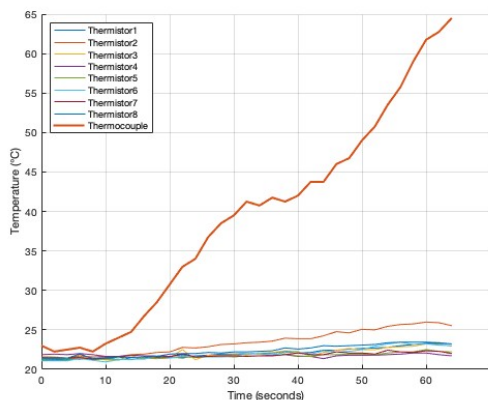


(b) Temperature profile at 1 minute 10 seconds.

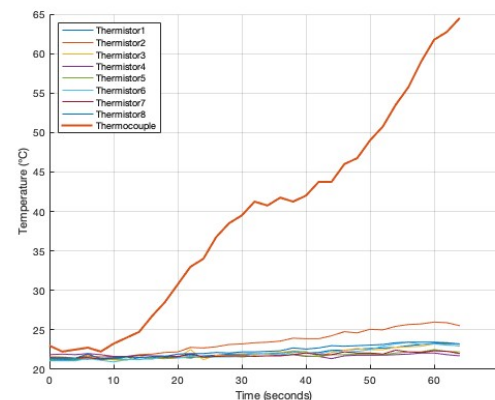
Figure 8.4: Temperature profiles with thermocouple placed at the bottom of the cavity (200W, FeAl₂O₃ catalyst).

8.5.2 Thermocouple at the Top of the Cavity

The thermocouple was then repositioned at the top of the cavity to observe any differences in temperature readings based on position. The following figures capture the temperature profiles when the thermocouple was placed at the top of the cavity.



(a) Temperature profile at 1 minute 0 seconds.



(b) Temperature profile at 1 minute 10 seconds.

Figure 8.5: Temperature profiles with thermocouple placed at the top of the cavity (200W, FeAl₂O₃ catalyst).

8.5.3 Infrared Thermogun Calibration

Figure 8.6 shows the Non-Contact Industrial Infrared Thermometer (Model: DT8380) used to confirm the accuracy of the thermocouple readings. The thermometer was aimed at different parts of the setup during microwave operation to ensure that the recorded temperature was reliable.



Figure 8.6: Non-Contact Industrial Infrared Thermometer displaying a reading used to confirm the thermocouple calibration during the experiment.

The calibration process indicated that the thermocouple provided accurate temperature readings in both positions (top and bottom of the cavity) during the experiment, with minor variations that were accounted for during the analysis.

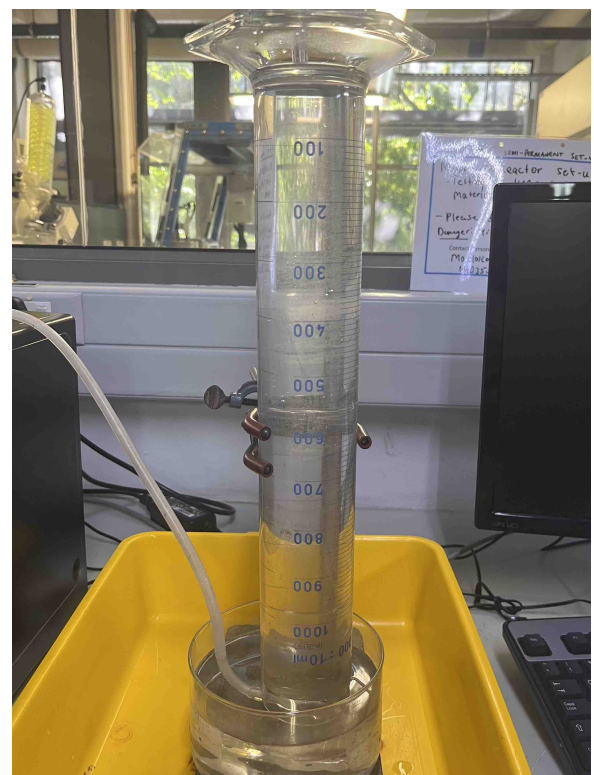
8.6 Inverter vs Transformer Additional Pictures

The following images display the catalyst after the various tests inside of the inverter microwave and the reaction flask at the beginning of the test for comparison.

8.6. Inverter vs Transformer Additional Pictures



(a) Catalyst after repeated tests.



(b) Start of the experiment setup.

Figure 8.7: Additional experimental setups and catalyst condition.

Chapter 9

Appendix B

9.1 Ethics Forms

This section includes the Ethics Pre-Screening Questionnaire Outcome Letter, confirming that no full ethics application is required for this project.



PRE-SCREENING QUESTIONNAIRE OUTCOME LETTER

STU-EBE-2024-PSQ001264

2024/08/13

Dear Caide Spiestersbach,

Your Ethics pre-screening questionnaire (PSQ) has been evaluated by your departmental ethics representative. Based on the information supplied in your PSQ, it has been determined that you do not need to make a full ethics application for the research project in question.

You may proceed with your research project titled:

Plastic to Power - Microwave Energy for Plastic Decomposition

Please note that should aspect(s) of your current project change, you should submit a new PSQ in order to determine whether the changed aspects increase the ethical risks of your project. It may be the case that project changes could require a full ethics application and review process.

Regards,

Faculty Research Ethics Committee